# The Organization and Animal–Vegetal Asymmetry of Cytokeratin Filaments in Stage VI *Xenopus* Oocytes Is Dependent upon F-Actin and Microtubules

**David L. Gard, Byeong Jik Cha, and Edward King**

*Department of Biology, University of Utah, Salt Lake City, Utah 84112*

**Confocal immunofluorescence microscopy with anti-cytokeratin antibodies revealed a continuous and polarized network of cytokeratin (CK) filaments in the cortex of stage VI *Xenopus* oocytes. In the animal cortex, CK filaments formed a dense meshwork that both was thicker and exhibited a finer mesh than the network of CK filaments previously observed in the vegetal cortex (Klymkowsky *et al.,* 1987). CK filaments first appeared in association with germinal vesicle (GV) and mitochondrial mass (MM) of oocytes in early mid stage I, indicating that CK filaments are the last of the three cytoskeletal networks to be assembled. By late stage I, CK filaments formed complex networks surrounding the GV, surrounding and penetrating the MM, and linking these networks to a meshwork of CK filaments in the oocyte cortex. During stage III–early IV, CK filaments formed a highly interconnected, apparently unpolarized, radial array linking the perinuclear and cortical CK filament networks. Polarization of the CK filament network was observed during mid stage IV–stage V, as first the animal, then the vegetal CK filament networks adopted the organization characteristic of stage VI oocytes. Treatment of stage VI oocytes with cytochalasin B disrupted the organization of both cortical and cytoplasmic CK filaments, releasing CK filaments from the oocyte cortex and inducing formation of numerous cytoplasmic CK filament aggregates. CB also disrupted the organization of cytoplasmic microtubules (MTs) in stage VI oocytes. Disassembly of oocyte MTs with nocodazole resulted in loss of the characteristic A–V polarity of the cortical CK filament network. In contrast, disruption of cytoplasmic CK filaments by microinjection of anti-CK antibodies had no apparent effect on cytoplasmic or MT organization. We propose a model in which the organization and polarization of the cortical network of CK filaments in stage VI *Xenopus* oocytes are dependent upon a hierarchy of interactions with actin filaments and microtubules.** © 1997 Academic Press

## INTRODUCTION

Stage VI *Xenopus* oocytes are polarized along an animal–vegetal (A–V) axis that is established during the later stages of oogenesis (reviewed in Gerhart, 1980; Gard, 1995). A–V polarity is externally apparent due to the asymmetric distribution of pigment in the oocyte cortex (Dumont, 1972). However, A–V polarity extends to many other structural features of the oocyte, including the distribution of yolk and the position of the oocyte nucleus, or germinal vesicle (GV). Recent studies have demonstrated that the cytoskeleton of stage VI *Xenopus* oocytes, which is composed of three major filamentous systems, microtubules (MTs) (Palecek *et al.,* 1985; Huchon *et al.,* 1988; Gard, 1991), actin microfilaments (F-actin) (Franke *et al.,* 1976; Roeder and Gard, 1994), and intermediate filaments (IFs) composed of cytokeratins (CKs) (Franz *et al.,* 1983; Godsave *et al.,* 1984; Klymkowsky *et al.,* 1987; Torpey *et al.,* 1992; Rya-

bova *et al.,* 1993), is also polarized along the A–V axis and may play a role in establishment or maintenance of oocyte polarity (for recent reviews, see Gard, 1995; Gard *et al.,* 1995c; Klymkowsky, 1995). Microtubules, for example, are more numerous in the animal hemisphere, where they are organized into loose bundles linking the GV to the oocyte cortex, while the sparser MT array of the vegetal cytoplasm exhibits little apparent order (Gard, 1991). Interestingly, the centrosomal protein $\gamma$-tubulin is asymmetrically distributed between the animal and vegetal cortices of stage VI *Xenopus* oocytes (Gard, 1994), suggesting that the oocyte cortex may play a role in regulating MT organization and polarity during oogenesis. Radially oriented actin cables have also been observed to link the GV to the animal cortex, while actin cables form a loose, three-dimensional network in the vegetal hemisphere (Roeder and Gard, 1994). Disruption of either MTs (Gard, 1991, 1993) or F-actin (Roeder and Gard, 1994) results in the displacement of the GV from its

normal position in the animal hemisphere, suggesting that both cytoskeletal systems play important roles in nuclear positioning. In addition, Yisraeli *et al.* (1990) demonstrated that the transport and anchoring of maternal Vg1 mRNA in the cortex of *Xenopus* oocytes constitute a two-step process requiring MTs and F-actin.

The organization and role of CK filaments during amphibian oogenesis and axis formation are less well known. Three CK polypeptides have been identified in *Xenopus* oocytes: two type I CKs and a single type II CK (Franz *et al.,* 1983; Franz and Franke, 1986; reviewed in Klymkowsky, 1995). Early studies using immunocytochemistry of sectioned oocytes with anti-CK antibodies revealed a sparse network of radially oriented CK filaments linking the GV to the animal cortex of stage VI oocytes (Franz *et al.,* 1983; Godsave *et al.,* 1984) and a more disordered CK filament array in the vegetal cytoplasm (Godsave *et al.,* 1984). In previtellogenic stage I oocytes, ''capsules'' of filaments surrounded the GV and mitochondrial mass (Godsave *et al.,* 1984). More recently, Klymkowsky and co-workers (1987) have observed a complex, anastomosing meshwork of CK filaments in the vegetal cortex of stage VI oocytes, while few CK filaments were apparent in the cortex of the animal hemisphere, indicating that the CK network of stage VI oocytes was polarized along the A–V axis. However, the relationship between assembly and polarization of the CK filament network and oocyte differentiation and polarization remained poorly documented.

The function of the CK network during oogenesis also has not been conclusively established. Previous studies (Klymkowsky *et al.,* 1992; Torpey *et al.,* 1992b) have shown that disruption of the maternal cytokeratin networks of early *Xenopus* embryos causes defects in gastrulation and wound healing during later development, leading to suggestions that the cytokeratins present in oocytes provide a pool of filament subunits used during later embryonic development. In addition, the CK filament networks present in oocytes might contribute to the structural support and elasticity of the oocyte cortex or play important roles in the transport and/or anchoring of developmentally important maternal RNAs in the oocyte cortex (Pondel and King, 1988; Elinson *et al.,* 1993; Forristall *et al.,* 1995).

Although MTs, F-actin, and CK filaments in *Xenopus* oocytes each exhibit a characteristic organization, there is substantial overlap in their distributions within the cytoplasm (for reviews, see Gard, 1995, Gard *et al.,* 1995b; Klymkowsky, 1995). For example, networks of all three cytoskeletal elements are present in the cortex, surround the GV, and appear to link the GV to the animal cortex (Palecek *et al.,* 1985; Huchon *et al.,* 1988; Gard, 1991; Franke *et al.,* 1976; Roeder and Gard, 1994; Franz *et al.,* 1983; Godsave *et al.,* 1984; Torpey *et al.,* 1992a; Ryabova *et al.,* 1993; Klymkowsky *et al.,* 1987). This overlap has led to suggestions that the cytoskeletal networks formed by F-actin, MTs, and CK filaments in *Xenopus* oocytes might interact or be physically linked (Gard, 1995; Klymkowsky, 1995), in a manner analogous to that proposed in many types of somatic cells. Supporting this hypothesis, results of preliminary studies

suggest that the organization of the microtubules, F-actin, and CK filaments in *Xenopus* oocytes are interdependent (Roeder and Gard, 1994; Gard *et al.,* 1995b; Klymkowsky, 1995). However, the interrelationship among the three cytoskeletal systems in *Xenopus* oocytes has not previously been examined in detail.

To better understand the biogenesis of the polarized network of CK filaments observed in *Xenopus* oocytes and the potential roles of CK filaments during specification and formation of the A–V axis, we have used anti-CK antibodies and confocal immunofluorescence microscopy to examine the distribution of CK filaments throughout oogenesis in *Xenopus.* In addition, to probe the interdependence of the three major elements of the oocyte cytoskeleton, we have examined both CK filament and MT organization in stage VI oocytes after disruption of F-actin, MTs, or CK filaments. The results presented support a model in which the organization and A–V polarity of the oocyte cytoskeleton are dependent upon a hierarchy of interactions between F-actin, MTs, and CK filaments. Interactions among these cytoskeleton systems may thus play an important role in the establishment and maintenance of the A–V polarity of *Xenopus* oocytes.

## MATERIALS AND METHODS

Juvenile (25–45 mm snout to vent) and adult *Xenopus laevis* were obtained from *Xenopus* I (Ann Arbor, MI). Ovaries and oocytes were collected as previously described (Gard, 1991; Gard *et al.,* 1995a).

### Disruption of the Oocyte Cytoskeleton with Cytochalasin B and MT Inhibitors

Stock solutions (10 mg/ml) of cytochalasin B (CB), nocodazole (NOC), colcemid, and vinblastine (all from Sigma Chemical Co., St. Louis, MO) were prepared in DMSO. Inhibitors were diluted to the indicated final concentrations in modified Barth's saline (MBSH: 88 m$M$ NaCl, 1 m$M$ KCl, 2.4 m$M$ NaHCO$_3$, 0.82 m$M$ MgSO$_4$, 0.33 m$M$ Ca(NO$_3$)$_2$, 0.4 m$M$ CaCl$_2$, 10 m$M$ Hepes, pH 7.4) immediately before use. CB and NOC were used at final concentrations of 1–20 $\mu$g/ml. Colcemid and vinblastine were used at final concentrations of 20 $\mu$g/ml. Oocytes were incubated in the indicated concentration of inhibitor for 2–48 hr at room temperature. Control oocytes were incubated for equivalent times in MBSH alone or in MBSH containing 0.05–0.4% DMSO.

### Disruption of Cytokeratin Filaments by Microinjection of Monoclonal Antibodies

C11 (specific for type I and II CKs, see below) and Tau-2 (specific for bovine brain tau protein) monoclonal ascites were obtained from Sigma Chemical Co. Tau-2 is the same isotype (IgG$_1$), and we have previously shown that *Xenopus* oocytes and eggs do not contain tau proteins (Gard and Kirschner, 1987; Gard, unpublished observation). SDS–PAGE revealed that IgG represented approximately 20% of the total protein in each ascites, with the remainder consisting largely of serum albumin. Ascites were diluted 1:1 with

injection buffer (IB: 50 m$M$ potassium glutamate, pH 7.2) and 25 $\mu$l of each was dialyzed for 3–5 hr against 25 ml of IB at 4°C. The ascites were further diluted with IB to concentrations that yielded 50–500 ng of total ascites protein in an injection volume of 50 nl, corresponding to approximately 10–100 ng of IgG (0.6–6 × 10$^{-13}$ mole) per oocyte. These amounts of IgG are comparable to those found by Klymkowsky *et al.* (1992) to disrupt CK organization in early *Xenopus* blastulae. Oocytes were incubated briefly in MBSH containing 5% Ficoll to reduce internal turgor pressure and were injected with approximately 50 nl of diluted ascites (C11 or Tau-2) or injection buffer alone. Injected oocytes were then transferred to MBSH and incubated 2–36 hr at room temperature, followed by fixation as described above.

## Immunofluorescence Microscopy of Cytokeratin Filaments and Microtubules

For visualization of cytokeratin filament organization, ovaries or oocytes were fixed in 100% methanol for 4–24 hr at room temperature. Microtubule organization was examined in oocytes fixed in FGT followed by postfixation in 100% methanol, as described previously (Gard, 1991, 1993b; Gard *et al.*, 1995c).

Ovaries and oocytes were rehydrated in Tris-buffered saline containing 0.2% NP-40 (TBSN). Ovaries from juvenile frogs were carefully dissected into small pieces (corresponding to one to two lobes of the ovary), to better expose the oocytes. Larger oocytes (stages III and larger) from adult frogs were hemisected, either laterally or along the equator, with a scalpel. The hemisected stage III–VI oocytes were then bleached (animal and vegetal hemispheres were bleached separately) in 30% H$_2$O$_2$:100% methanol (1:2) and were processed for immunofluorescence as previously described (Gard, 1993b; Gard *et al.*, 1995c).

Two monoclonal antibodies were used to stain cytokeratin filaments. Monoclonal 1h5 (generously provided by Dr. Michael Klymkowsky; used at 1:50 dilution) recognizes the single type II cytokeratin of *Xenopus* oocytes (which is most closely related to human CK-8) as well as two soluble proteins (Klymkowsky *et al.*, 1987). The ''pan-cytokeratin'' monoclonal C11 (catalog No. C-2931; Sigma Chemical Co.; used at 1:200 dilution) recognizes human CK-8 and other members of both type I and type II cytokeratin families in epithelial cells of many species, including *Xenopus* (Bartek *et al.*, 1991; Staskova *et al.*, 1991). Western immunoblots revealed that 1h5 and C11 antibodies recognized the single 54-kDa type II CK found in *Xenopus* oocytes (not shown; Franz *et al.*, 1983; Franz and Franke, 1988).

Microtubules were stained with DM1A (specific for $\alpha$-tubulin; diluted 1:100) (ICN Immunochemicals, Lisle, IL) or 6-11B-1 (specific for acetylated $\alpha$-tubulin; diluted 1:100) (Sigma Chemical Co.). Secondary antibodies were obtained from Cappell (rhodamine- or fluorescein-conjugated anti-mouse IgGs; Cappell, Malvern, PA) or Molecular Probes (Texas-red-conjugated anti-mouse IgG; Molecular Probes, Eugene, OR).

Chromosomes of stage 0 oocytes and follicle cells were labeled with ethidium homodimer (EH) or Yo Pro-1 (YP; 1–5 $\mu$g/ml; Molecular Probes) in 100% methanol during the final dehydration prior to clearing with benzyl alcohol:benzylbenzoate (1:2) (Gard, 1993b; Gard *et al.*, 1995c).

## Confocal Microscopy and Three-Dimensional Volume Reconstruction and Rendering from Confocal Images

Single and serial optical sections were collected using a Bio-Rad MRC-600, as described previously (Gard, 1991, 1993b; Gard *et al.*,

1995c). For many images, increased depth of focus was achieved by projecting 2–38 serial optical sections, using a maximum brightness algorithm. 3-D reconstruction and rendering of oocytes (up to 76 optical sections) were performed using VoxBlast software (Vaytek; Fairfield, IA) running on a 90-MHz Pentium equipped with 64 MB of RAM. The opacity and color look-up tables were adjusted for each Z-series, in order to render the cytoplasm and nuclear volume transparent while revealing the CK filaments. In some 3-D reconstructions, the surface contour of the GV was approximated by tracing the nuclear margin in two-dimensional sections at intervals of 1–3 $\mu$m. Stereo pairs were generated by rendering oocytes from two viewing angles that differed by 6° in azimuth.

## Electron Microscopy of Cytochalasin-Treated Oocytes

CB-treated oocytes were fixed in a combination of 3.2% paraformaldehyde (EM Sciences; Fort Washington, PA) and 3% glutaraldehyde (Ted Pella, Inc.; Redding, CA) in 50 m$M$ sodium cacodylate buffer containing 100 m$M$ KCl, 1 m$M$ MgCl$_2$, 5 m$M$ EGTA, and 1% sucrose in glass-distilled H$_2$O (dH$_2$O) for 4 hr at room temperature and then overnight at 40C. Fixed oocytes were rinsed in dH$_2$O and hemisected. The vegetal hemispheres were washed three times (1 hr each) in 1% sucrose in dH$_2$O, followed by postfixation for 3 hr in aqueous 1% OsO$_4$ containing 1% sucrose. Specimens were then washed 3 hr in 1% sucrose, stained with 1% aqueous uranyl acetate for 1 hr, washed 2 hr in dH$_2$O, and dehydrated in ethanol (30–100%). Specimens were embedded in Araldite:Embed 812 (EM Sciences). Thin sections (90 nm) were stained with 1% aqueous uranyl acetate and with Reynolds' lead citrate (Reynolds, 1963) and examined in a Hitachi H-7100 electron microscope.

# RESULTS

## A Polarized Network of Cytokeratin Filaments Extends throughout the Cortex of Stage VI Xenopus Oocytes

Monoclonal anti-cytokeratin antibodies 1h5 and C11 (see Materials and Methods) were used to examine the distribution of cytokeratin filaments in oocytes from juvenile (20–45 mm snout to vent) and adult *Xenopus laevis.* Both 1h5 (not shown) and C11 antibodies revealed a complex network of anastomosing CK filaments[1] in the vegetal cortex of stage VI *Xenopus* oocytes (Fig. 1A), as previously described by Klymkowsky and co-workers (1987). Such CK networks were observed in the vegetal cortex of 94% (208 of 221) of the oocytes obtained from 18 different females.

Confocal immunofluorescence microscopy of stage VI oocytes stained with 1h5 or C11 antibodies also revealed ex-

---

[1] The apparent diameter of the CK ''filaments'' revealed by confocal immunofluorescence microscopy was approximately 0.4–0.5 $\mu$m, which is consistent with the diffraction-limited resolution limit of the objective and excitation wavelength used during imaging. Due to this resolution limit, it is not possible to determine whether the observed structures represent individual CK filaments (with diameters of 9–12 nm) or filament bundles using confocal microscopy.
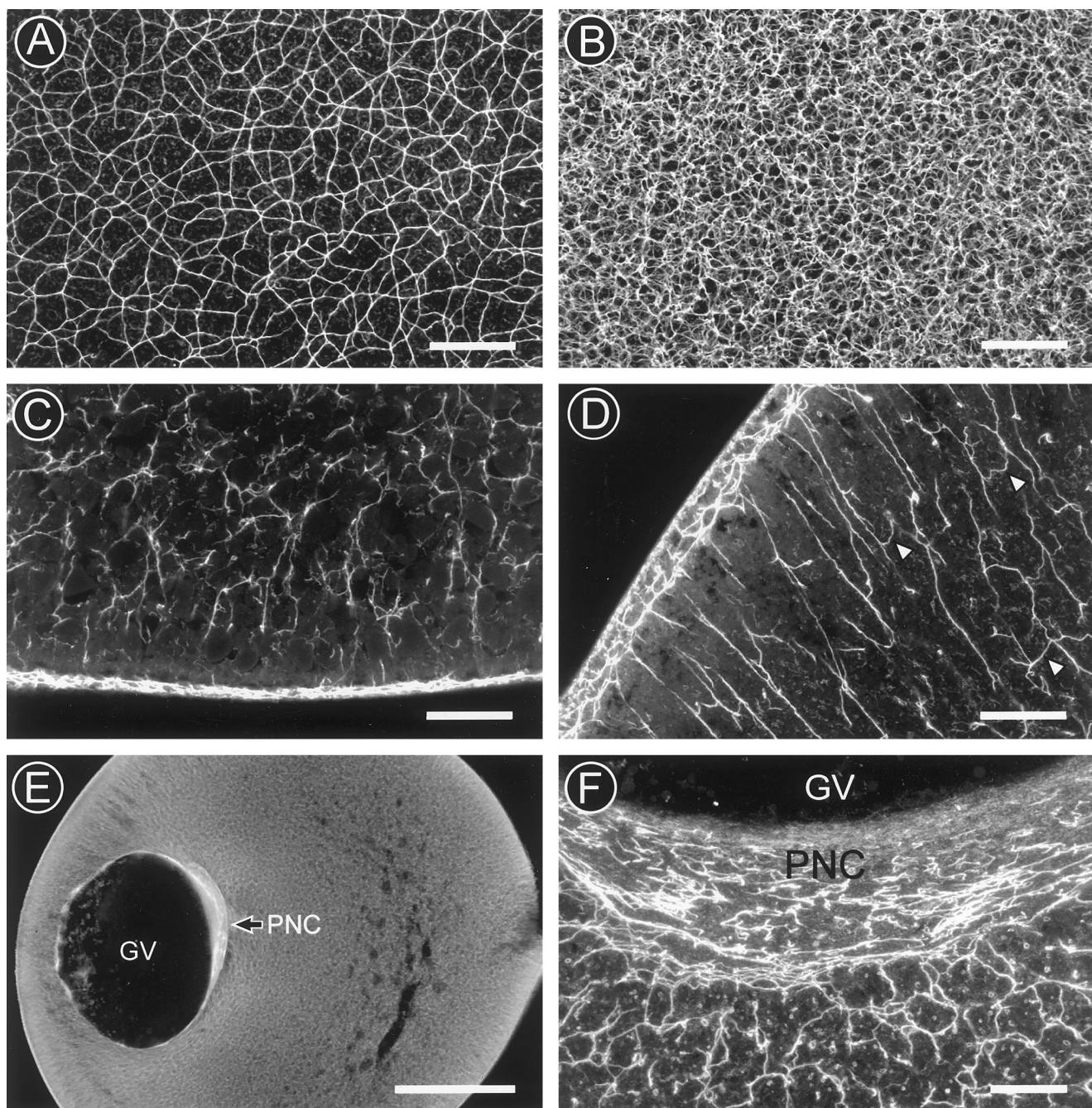
**FIG. 1.** Confocal immunofluorescence microscopy of stage VI oocytes reveals a complex network of cytokeratin filaments in the animal and vegetal cortices. (A and B) Grazing views (projections of four and five sections at 1-$\mu$m intervals, respectively) of the vegetal (A) and animal (B) cortices of stage VI oocytes stained with C11 antibodies reveal complex networks of CK filaments in the cortices of both hemispheres. Note the characteristic difference in complexity and apparent mesh size of CK networks in the vegetal and animal cortices. (C and D) Optical cross sections (projections of five serial sections collected at 1-$\mu$m intervals) of the vegetal (C) and animal (D) hemispheres revealed the cortical CK filament networks, as well as a substantial network of CK filaments in the underlying subcortical cytoplasm. Note the difference in thickness of the cortical CK network in the vegetal and animal cortices and the radial organization of CK filaments in the animal hemisphere. Arrowheads in D denote transverse CK filaments (see text). (E) A low-magnification view (a single section) of an oocyte stained with C11 antibodies reveals an extensive network of CK filaments extending throughout the cytoplasm and surrounding the germinal vesicle (GV) and perinuclear cap of yolk-free cytoplasm (PNC). (F) Numerous CK filaments are apparent in this high-magnification image of the perinuclear cap of yolk-free cytoplasm (PNC) (a projection of five sections collected at 1-$\mu$m intervals). Scale bars are 25 $\mu$m in A–D, and F and 250 $\mu$m in E.

tensive networks of CK filaments in the animal cortex, which were most evident in projections of 5–15 serial optical sections (Fig. 1B). Such networks were observed in the animal cortex of 96% (223 of 232) of the stage VI oocytes examined from 18 different females. However, the apparent "mesh" size of the CK filament network in the animal cortex was notably "finer" than that observed in the vegetal cortex (compare Figs. 1B and 1A), and the CK filament network of the animal cortex appeared more highly interconnected. In grazing sections of the lateral cortex, a visible transition from the finer CK meshwork of the animal cortex to the coarser network of the vegetal cortex appeared to roughly coincide with the oocyte equator (not shown). Serial optical sectioning suggested that the CK filament networks observed in animal cortices of stage VI oocytes extended further into the cortical and subcortical cytoplasm, and were more complex and interconnected, than those observed in vegetal cortices. This difference was confirmed in optical cross sections (Figs. 1C and 1D), in which the cortical CK filament network of the animal cortex (Fig. 1D) was typically two- to threefold thicker (averaging $8.0 \pm 2.7$ $\mu$m; $n = 58$) than that observed in the vegetal cortex ($3.3 \pm 0.8$ $\mu$m; $n = 43$) (Fig. 1C).

Cross sections also revealed a complex and polarized network of CK filaments extending throughout the cytoplasm of both vegetal (Fig. 1C) and animal (Fig. 1D) hemispheres of stage VI oocytes. In the animal hemisphere, a mesh of CK filaments surrounded the GV and extended throughout the cap of yolk-free cytoplasm apposed to its basal surface (Figs. 1E–1F). Radially oriented CK filaments linked the perinuclear CK meshwork to the overlying network of CK filaments in the animal cortex (Fig. 1D), as previously described (Franz *et al.,* 1983; Godsave *et al.,* 1984; Torpey *et al.,* 1992a; Ryabova *et al.,* 1993). Projections of serial cross sections (as in Fig. 1D) and three-dimensional reconstructions (not shown) revealed a population of transversely oriented CK filaments (arrowheads in Fig. 1D) connecting adjacent radial filaments. In the vegetal cytoplasm, CK filaments appeared less ordered (Fig. 1C). Estimates of the number of CK filaments passing through optical sections collected 5–10 $\mu$m below the oocyte surface indicated that a single oocyte contained 9000–15,000 radially oriented cytoplasmic CK filaments.[2]

### The Network of Cytoplasmic Cytokeratin Filaments First Appears in Mid Stage I of Oogenesis

To more fully understand their potential roles during oogenesis, the organization of CK filaments was examined during early oogenesis in juvenile and adult frogs. Examination of ovaries from small juvenile frogs (20–30 mm snout

to vent) stained with either 1h5 or C11 antibodies revealed that CK filaments were confined to the surrounding follicle tissue and were absent from oocytes in stage 0–early stage I of oogenesis (Figs. 2A–2B) (stage 0 refers to prediplotene oocytes; see Gard *et al,* 1995a,c). "Nests" of stage 0 oocytes were recognized by the characteristic "bouquet" organization of their chromosomes (Al-Mukhtar and Webb, 1971; Coggins, 1973; Gard *et al.,* 1995a), revealed by the DNA-binding dyes EH or YP (red channel in Fig. 2A). Such nests typically were surrounded by follicle cells that stained brightly with either 1h5 (not shown) or C11 antibodies (green channel in Fig. 2A). However, no CK-staining was detectable within the stage 0 oocytes themselves. Similarly, larger individual stage 0 oocytes (Fig. 2B) and early stage I oocytes (not shown) were surrounded by follicle cells that stained brightly with C11 anti-CK antibodies, but themselves lacked detectable cytoplasmic CK filaments.

Cytoplasmic CK filaments (see footnote 1) were first apparent in mid stage I oocytes (75–125 $\mu$m) obtained from slightly larger juvenile frogs (30–45 mm snout to vent) (Fig. 2C is a stereo pair showing CK filament organization in a 125-$\mu$m oocyte). CK filaments were first observed to form a perinuclear network surrounding the GV and one or more perinuclear mitochondrial aggregates (M in Fig. 2C). The extent and complexity of the perinuclear network of CK filaments increased during mid stage I, such that the largest oocytes examined from juvenile frogs (approx. 150–175 $\mu$m in diameter) contained extensive networks of CK filaments surrounding the GV, surrounding and penetrating the mitochondrial mass (by this stage, most oocytes contained a single mitochondrial mass; Gard *et al.,* 1995a), and extending from the perinuclear network into the surrounding cytoplasm (Fig. 2D). Perinuclear, cytoplasmic, and cortical CK filaments first became apparent in oocytes from adult frogs during mid stage I, in oocytes with diameters greater than 100 $\mu$m. By mid–late stage I (greater than 150 $\mu$m in diameter), the GV was surrounded by a perinuclear network of CK filaments, and a poorly ordered network of cytoplasmic CK filaments linked the perinuclear network to CK filaments in the oocyte cortex (Fig. 3A). CK filaments also were concentrated in a complex network associated with the mitochondrial mass (M in Figs. 3A and 3B), both surrounding and penetrating this aggregate of organelles, and linking it to both perinuclear and cortical CK networks. By late stage I–stage II (250–400 $\mu$m in diameter), a dense, poorly ordered network of CK filaments was observed to extend throughout the cytoplasm (Fig. 3C), linking the GV to CK filaments in the cortical cytoplasm (arrowheads in Fig. 3C).

### Polarization of the Cortical and Cytoplasmic CK Network Occurs during Mid Stage IV

Stage III of oogenesis is marked by the accumulation of pigment in the oocyte cortex, which initially is distributed symmetrically throughout the oocyte cortex (Dumont, 1972). During early stage III (>400 $\mu$m in diameter.), CK filaments in the peripheral cytoplasm were observed in a

---

[2] Based upon estimates of the number of radially oriented CK filaments in the animal and vegetal hemispheres (approximately 10 per 1000 $\mu$m$^2$ and 6 per 1000 $\mu$m$^2$ of surface area, respectively) and a total surface area of $1.5 \times 10^6$ $\mu$m$^2$ per oocyte.
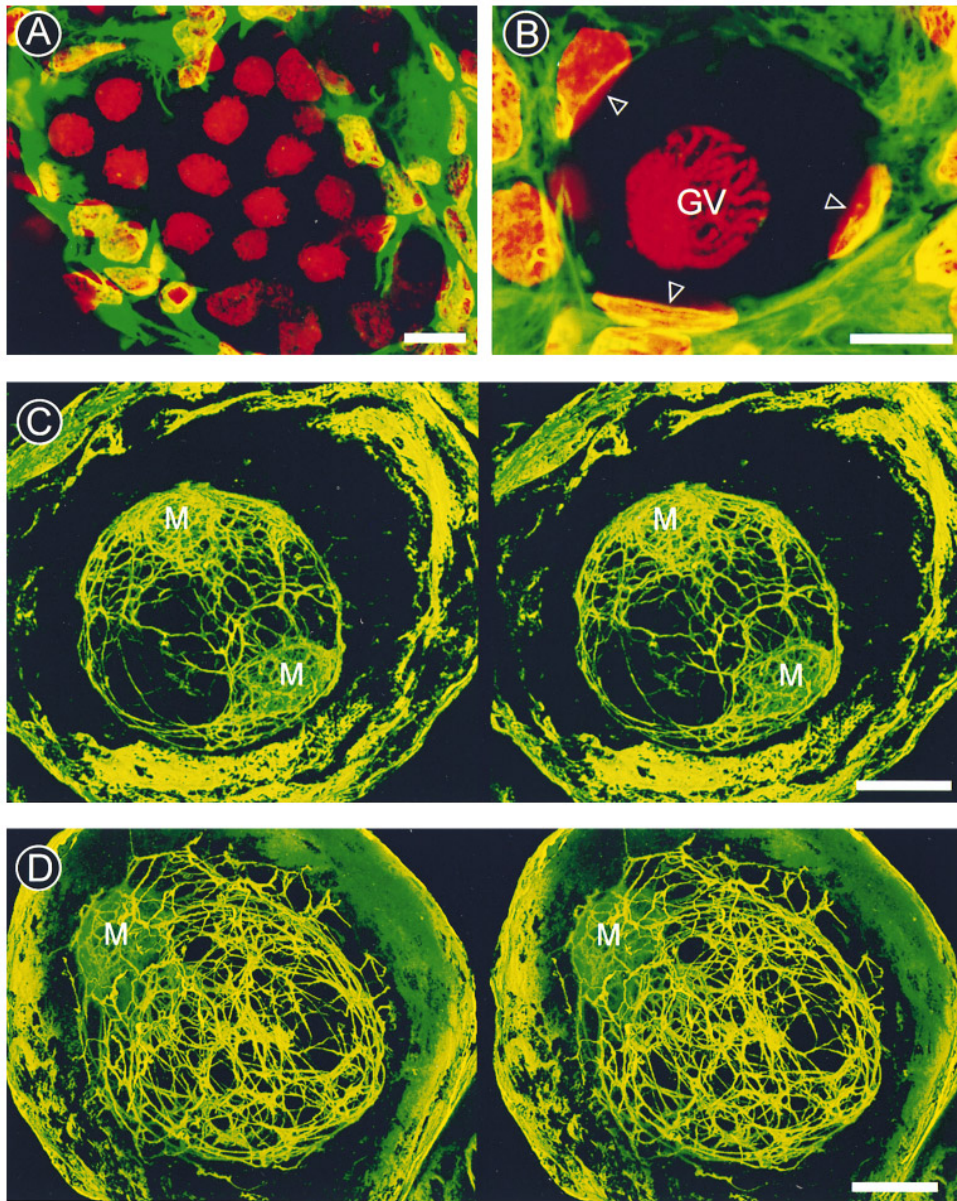
**FIG. 2.** Cytokeratin filaments are first apparent during mid stage I of oogenesis. (A) A nest of early stage 0 oocytes isolated from a juvenile frog and stained with C11 antibodies (green) and EH (red). Cytokeratin staining is apparent only in the follicle cells surrounding the oocytes. A projection of 3 optical sections. (B) A single late-stage 0 oocyte (35-$\mu$m diameter) isolated from a juvenile frog and stained with C11 antibodies (green) and YP (red). Cytokeratin staining is apparent only in the surrounding follicle cells (arrowheads denote follicle cell nuclei). Note the characteristic ''bouquet'' organization of a chromatin. A projection of 3 optical sections. (C) A stereo view of a mid stage I (125-$\mu$m diameter) oocyte from a juvenile frog stained with C11, showing the assembly of a perinuclear CK filament network and the association of CK filaments with two mitochondrial aggregates (M). Note the lack of cytoplasmic and cortical CK filaments. Reconstructed from 53 optical sections. (D) A stereo view of a mid–late-stage I (150 $\mu$m) oocyte from a juvenile frog stained with C11 antibodies. Note the extensive perinuclear network of CK filaments, the CK filaments associated with the mitochondrial mass (M), and individual filaments extending from the perinuclear network into the surrounding cytoplasm. Reconstructed from 70 optical sections. Scale bars are 10 $\mu$m in A and B and 25 $\mu$m in C and D.

more radial organization (arrowheads in Fig. 4A). These ''radial'' CK filaments appeared to link CK filaments in the cortex to a dense, less ordered network of CK filaments in the yolk-free cytoplasm surrounding the GV.

During stage IV of oogenesis, pigment becomes concentrated in the animal cortex, providing the first external evidence of the A–V axis (Dumont, 1972). Despite visible polarization of the pigment distribution, no A–V polarization
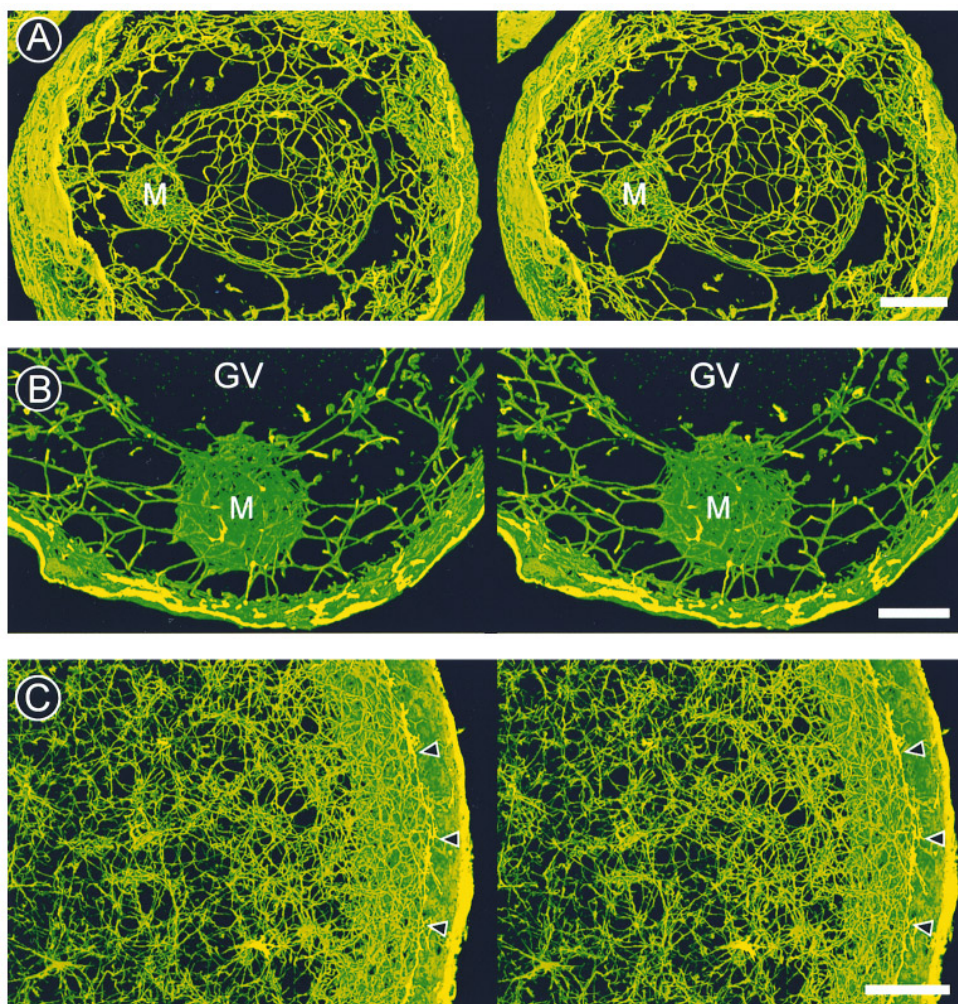
**FIG. 3.** Cytokeratin filaments form perinuclear, cytoplasmic, and cortical networks during stages I and II of oogenesis. (A) A stereo view of a late stage I (185-$\mu$m diameter) oocyte isolated from an adult frog stained with C11 antibodies, showing a meshwork of CK filaments surrounding the GV and linking the GV and mitochondrial mass (M) to the oocyte cortex. Reconstructed from 76 optical sections. (B) A stereo pair of the mitochondrial mass of a stage I oocyte (approximately 200 $\mu$m in diameter) isolated from an adult frog and stained with C11 antibodies (reconstructed from 25 optical sections). Note the extensive network of CK filaments surrounding and filling the mitochondrial mass. (C) A stereo view of a late stage II or early stage III (350–400 $\mu$m in diameter) oocyte. Little radial order is seen in the cytoplasmic CK network. The dense, subcortical CK network (arrowheads) lies approx. 10 $\mu$m below the oocyte surface. Reconstructed from 39 optical sections. Scale bars are 25 $\mu$m.

was apparent in the organization of cytoplasmic or cortical cytokeratin filaments during early stage IV (450–500 $\mu$m in diameter; Figs. 4B and 4C show animal and vegetal regions of the same oocyte). CK filaments were observed to extend radially from a dense CK filament network in the yolk-free region surrounding the GV (which was still centered in the oocyte cytoplasm) toward a complex CK filament network in the oocyte cortex. 3-D reconstructions (Figs. 4B and 4C) revealed an additional population of CK filaments linking adjacent radially oriented CK filaments, giving the entire CK filament network the appearance of a vast, spherically symmetric, "Jacob's ladder" linking the GV to the cortex.

Polarization of the cortical and cytoplasmic CK filament network was first apparent during mid stage IV of oogenesis (600–800 $\mu$m in diameter) (Fig. 5). Surprisingly, the CK network in the vegetal cortex of mid stage IV oocytes was observed to be two- to threefold thicker than that of the animal cortex (Figs. 5A and 5B), the opposite of the cortical CK filament distribution in stage VI oocytes (compare Fig. 5B to Figs. 1C and 1D). A visible transition in the thickness of the cortical CK network (seen in Figs. 5A and 5B) roughly corresponded in position to the oocyte equator. Grazing sections of the animal and vegetal cortex also revealed the A–V polarity of the cortical CK network by mid stage IV (Figs.
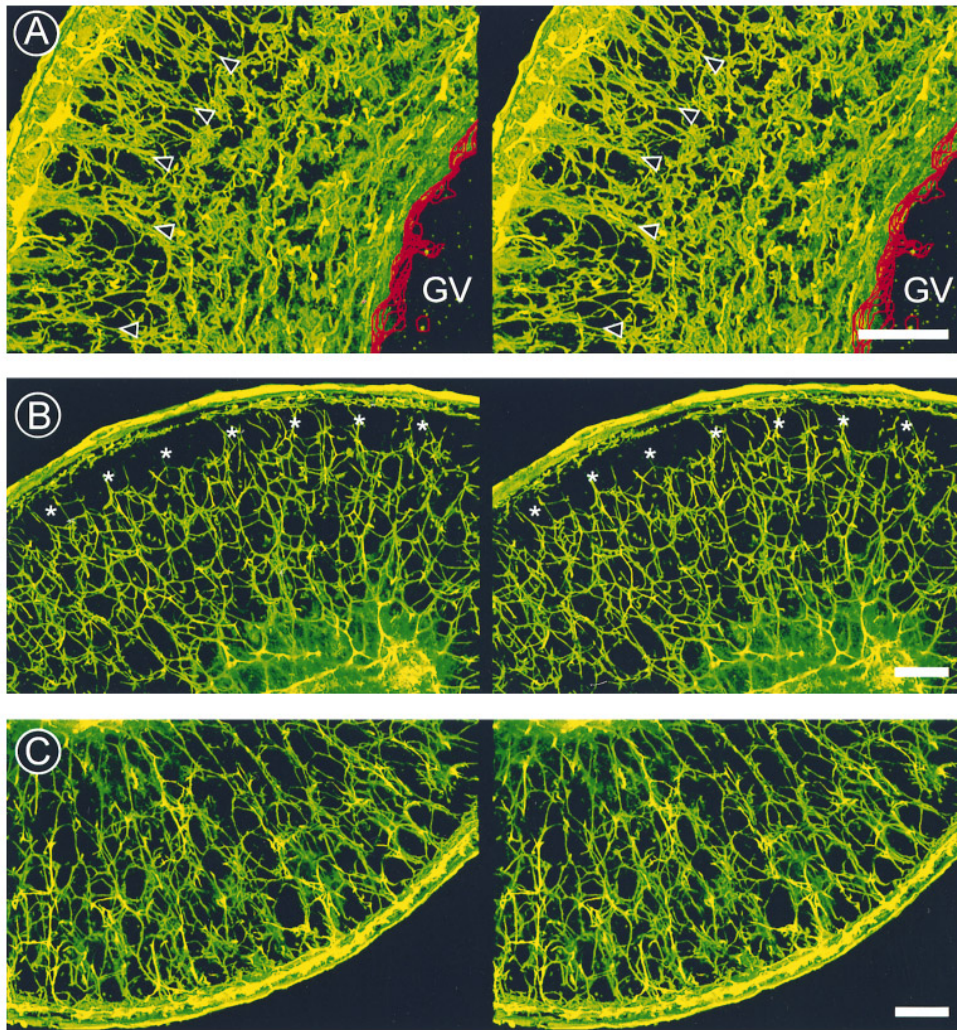
**FIG. 4.** The CK filament network of early stage IV oocytes is not detectably polarized along the A–V axis. (A) A stereo view of a stage III oocyte (approx. 400 $\mu$m in diameter). Radially oriented CK filaments (arrowheads) link the cortical CK network to a less-ordered CK network surrounding the GV (outlined in red). Reconstructed from 20 optical sections. (B,C) Stereo views (both reconstructed from 15 optical sections) of the animal (B) and vegetal (C) regions of a single early stage IV oocyte (450–500 $\mu$m in diameter). No evidence of polarity is seen in the organization of cytoplasmic or cortical CK filaments in these views of the same oocyte. Note the numerous transverse connections between the radially oriented CK filaments in all three views. Asterisks in B denote obscuration of the CK filaments in the subcortical region of the animal hemisphere due to accumulation of pigment. Scale bars are 25 $\mu$m.

5C and 5D). In the animal hemisphere (Fig. 5C), the cortical CK network exhibited a fine, three-dimensional meshwork that approached the appearance of that observed in the animal cortex of stage VI oocytes. While the network of CK filaments in the vegetal cortex of mid stage IV oocytes exhibited a coarse network with a mesh size similar to that observed in the vegetal cortex of stage VI oocytes (compare Fig. 5D to Fig. 1A), serial grazing sections (not shown) and cross-sections (Fig. 5B) revealed that the stage IV network was much thicker (deeper) than the corresponding network in the vegetal cortex of stage VI oocytes. "Maturation" of the CK network in the vegetal cortex to the thin, open meshwork observed previously in the vegetal cortex of stage VI oocytes (Klymkowsky *et al.,* 1987; Figs. 1C and 1D) was not apparent until oocytes reached diameters of 1000–1100 $\mu$m (stage V).

The A–V asymmetry of the cytoplasmic CK filaments was also apparent by mid stage IV (Fig. 5B). In the animal hemisphere, CK filaments retained the radial orientation apparent during stage III–early stage IV, extending from the GV to the cortical CK network. In the vegetal hemisphere, the cytoplasmic CK filaments exhibited less radial order. The organization and A–V asymmetry of cytoplasmic CK filaments observed during mid–late stage IV were thus sim-

ilar to those observed in fully grown stage VI oocytes (compare Fig. 5B to Figs. 1C and 1D).

### *Cytochalasin B Disrupts CK Filaments and MT Organization in Xenopus Oocytes*

Previous studies have demonstrated that *Xenopus* oocytes contain complex cortical and cytoplasmic networks of actin cables (Franke *et al.,* 1976; Roeder and Gard, 1994) and MTs (Palecek *et al.,* 1985; Huchon *et al.,* 1988; Gard, 1991). To explore the interrelationships among F-actin, MTs, and CK filaments, we examined the organization of CK filaments and MTs in stage VI oocytes which were treated for 2–48 hr with cytochalasin B (CB; 1–20 $\mu$g/ml) (see Materials and Methods). Previous studies have demonstrated that these concentrations of CB are sufficient to substantially disrupt both cytoplasmic and cortical F-actin in stage VI *Xenopus* oocytes (Roeder and Gard, 1994; Gard *et al.,* 1995b; see Coleman *et al.,* 1981, and Roeder and Gard, 1994, for discussions of the effects of CB on oocyte morphology), without blocking progesterone-induced GV breakdown (Ryabova *et al.,* 1986; Gard *et al.,* 1995b).

Extended incubation of stage VI oocytes in CB resulted in dramatic reorganization of cortical and cytoplasmic CK filaments (Fig. 6). After 20 hr, optical cross sections of CB-treated oocytes revealed that the CK filaments had been released from the cortex or stretched into the subcortical cytoplasm of both animal (Fig. 6A) and vegetal (not shown) hemispheres. Release of the CK filaments from the cortex and stretching of the CK network into the subcortical cytoplasm were apparent as soon as 6 hr after addition of 1–20 $\mu$g/ml CB, and by 48 hr, CK filaments were often observed to be stretched 40–50 $\mu$m into the subcortical cytoplasm of the animal hemisphere and 25–35 $\mu$m into the vegetal hemisphere. Most CB-treated oocytes contained numerous, tightly curled, tangles of CK filaments in the subcortical cytoplasm, which were typically located near the interior margin of the distorted network of cortical CK filaments (arrowheads in Fig. 6A). These CK filament tangles were apparent in projections of tangential optical sections of the cortical and subcortical cytoplasm of CB-treated oocytes (arrowheads in Fig. 6B). Tangential sections also often revealed fibrous aggregates of CK filaments in the cortex of CB-treated oocytes (arrow in Fig. 6B).
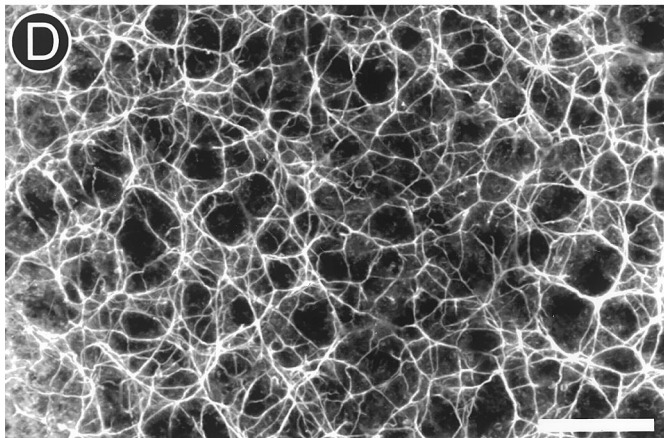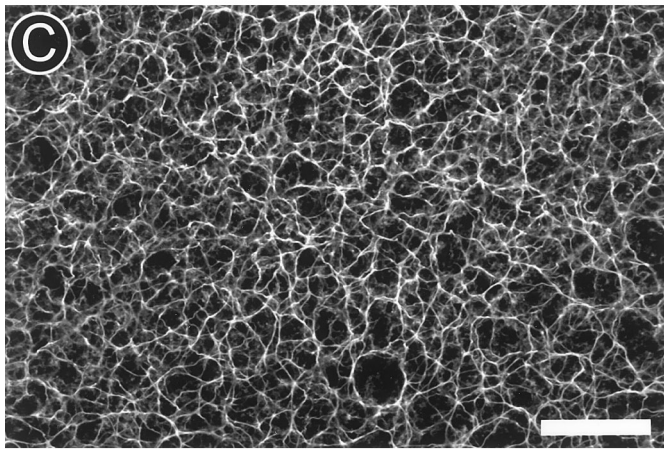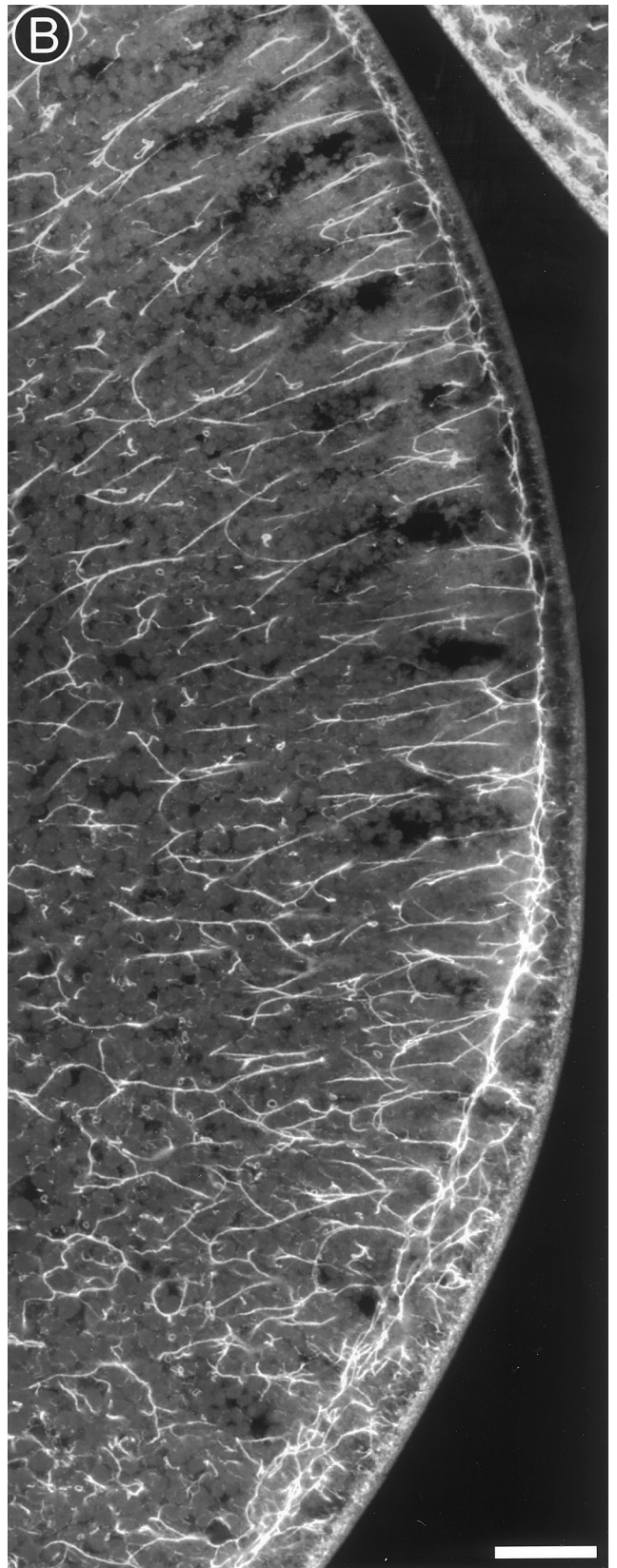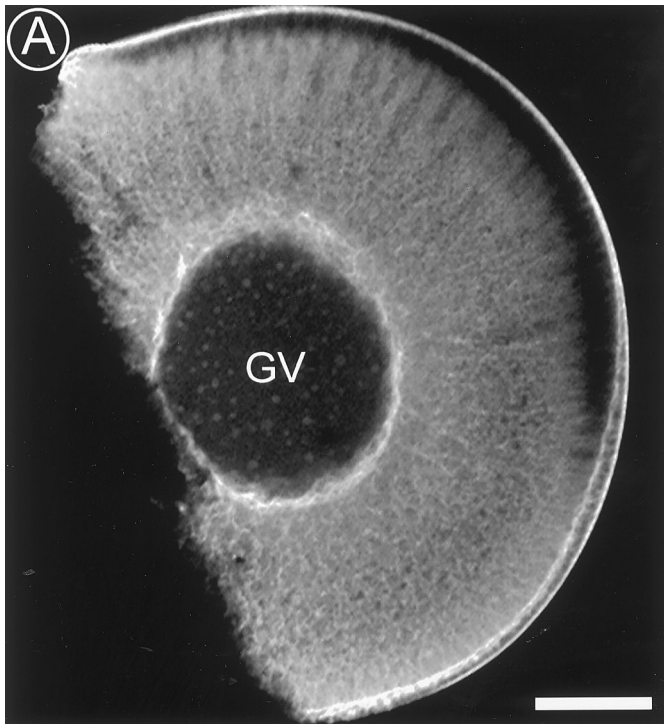
Treatment of stage VI oocytes with 1–20 $\mu$g/ml CB also resulted in the formation of numerous globular and fibrous cytoplasmic aggregates that stained brightly with C11 antibodies (Figs. 6C and 6D). These CK aggregates were apparent as early as 6 hr after addition of CB and were observed throughout the oocyte cytoplasm, although they were often clustered beneath the GV (Fig. 6C). Transmission electron microscopy of oocytes treated with CB for 20 hr (not shown) revealed that the CK aggregates observed in CB-treated oocytes contained numerous, densely packed filaments with a mean diameter of 9.5 nm ($\pm$1.8 nm, $n$ = 53), consistent with the reported diameter of cytokeratin intermediate filaments in other cell types (see Goldman and Steinert, 1990, and references therein). The number, location, morphology,

and time of appearance of the brightly-stained CK aggregates were similar to those of F-actin-containing aggregates previously observed in CB-treated oocytes stained with fluorescent phalloidin (Roeder and Gard, 1994) (compare Figs. 6D and 6E). However, incompatibility of the fixation protocols for visualizing CK filaments and F-actin prevented direct confirmation by confocal fluorescence microscopy that CK filaments and F-actin were contained within the same aggregates. The dramatic reorganization of cortical CK filaments observed in CB-treated oocytes was not apparent in oocytes incubated for comparable periods in MBSH containing 0.2% DMSO, which appeared indistinguishable from oocytes incubated in MBSH alone.

We also compared MT organization and acetylation in untreated (or DMSO-treated) stage VI oocytes with those observed in oocytes treated with 1–20 $\mu$g/ml CB for up to 48 hr. Untreated stage VI oocytes (or those incubated in 0.2% DMSO) contain characteristic, radially oriented MT bundles in the animal hemisphere, which stain brightly with monoclonal 6-11B-1 antibodies to acetylated $\alpha$-tubulin (arrows in Fig. 6F) (Gard, 1991), a marker for stable MTs (Piperno *et al.,* 1987; Schulze *et al.,* 1987; Webster *et al.,* 1989). A less-ordered array of cytoplasmic MTs, containing fewer acetylated MTs, is present in the vegetal hemisphere (not shown; Gard, 1991). Extended incubation in 1–20 $\mu$g/ml CB resulted in a progressive disruption of normal MT organization (Fig. 6G), including loss of the radial array of MT bundles in the animal hemisphere and the appearance of a broad band of disordered MTs in the subcortical regions of both animal (arrows in Fig. 6G) and vegetal hemispheres (not shown). These disordered MTs were brightly stained by either DM1A (specific for total $\alpha$-TB) (not shown) or 6-11B-1 antibodies specific for acetylated $\alpha$-tubulin (Fig. 6G). Staining of the disordered MTs in CB-treated oocytes with antibodies to acetylated tubulin suggests that CB does not stimulate *de novo* MT assembly, but rather disorganizes the preexisting MT array. MT organization was unaffected by incubation for comparable periods of time in 0.1–0.2% DMSO.

### *The Animal–Vegetal Polarity of Cortical Cytokeratins in Stage VI Xenopus Oocytes Is Disrupted by Microtubule Inhibitors*

To determine whether the organization of CK filaments in *Xenopus* oocytes was dependent upon microtubules, we examined the organization of CK filaments in oocytes incubated in the MT inhibitor NOC (1–20 $\mu$g/ml) for periods ranging from 2 to 48 hr. Treatment with NOC resulted in the disassembly of nearly all cytoplasmic MTs within 2 hr, and no MTs could be detected after longer incubations (up to 48 hr) (data not shown; Gard, 1991). Confocal immunofluorescence microscopy with C11 anti-CK antibodies revealed that disruption of the oocyte MT cytoskeleton with NOC had a dramatic effect on the organization of the cortical CK network of stage VI oocytes. CK filament networks in both the vegetal (Fig. 7A) and the animal (Fig. 7B) cortex of NOC-treated oocytes exhibited a very fine mesh (com-

pare Figs. 7A and 7B with 1A and 1B, which are presented at the same image scale and include the entire depth of the cortical CK network).

Serial grazing sections (not shown) of the cortex of NOC-treated oocytes suggested that treatment with NOC also eliminated the distinct A–V asymmetry observed in the thickness of the CK networks of the animal and vegetal cortices of untreated oocytes. This conclusion was confirmed by optical cross sections of the vegetal (Fig. 7C) and animal (Fig. 7D) cortices of NOC-treated oocytes, which exhibited a nearly uniform thickness of 2–4 $\mu$m (compare Figs. 7C and 7D to Figs. 1C and 1D). Reorganization of the cortical CK filament network was first apparent 4–6 hr after addition of 5–20 $\mu$g/ml of NOC, and maximum effects were observed by 15–24 hr. Similar effects were also observed in oocytes treated with concentrations of NOC as low as 1 $\mu$g/ml (for 20–24 hr) and in oocytes incubated for 6–20 hr in either vinblastine (20 $\mu$g/ml) or colcemid (20 $\mu$g/ml) (not shown).

Incubation of stage VI oocytes in combinations of NOC and CB for extended periods resulted in severe stratification of cytoplasm, rupture of the GV, and other cytological changes suggestive of cell death (not shown), which were only rarely observed in oocytes treated with either CB or NOC alone. Better survival (>75%) was obtained at lower inhibitor concentrations (5 $\mu$g/ml CB and 1–5 $\mu$g/ml NOC) for shorter periods of time (<20 hr), though substantial alterations in pigment and yolk distribution were still evident (not shown). Examination of CK filament organization in these oocytes revealed that inclusion of NOC at concentrations of 1–5 $\mu$g/ml inhibited the release and/or inward stretching of the cortical CK network observed in oocytes treated with 5 $\mu$g/ml CB alone (compare Figs. 7E and 7F with Fig. 6A), suggesting that the inward stretching of cortical CK filaments in CB-treated oocytes is dependent upon MTs.

### Microtubule Organization in Stage VI Xenopus Oocytes Is Not Dependent on Cytoplasmic Cytokeratin Filaments

To determine whether MT organization was dependent upon cytoplasmic CK filaments, we examined MT organization in stage VI oocytes after disruption of their CK networks. Previous studies have shown that microinjection of cytokeratin antibodies disrupts CK filament organization in cultured epithelial cells (Klymkowsky *et al.,* 1983) and early *Xenopus* embryos (Klymkowsky *et al.,* 1992). We thus injected stage VI oocytes with 10–100 ng of C11 monoclonal antibodies and examined the distribution of CK filaments and MTs by confocal immunofluorescence microscopy. Control oocytes were injected with comparable amounts of injection buffer or anti-tau antibodies (see Materials and Methods).

Microinjection of C11 antibodies resulted in a dose- and time-dependent disruption of the cytoplasmic network of CK filaments of stage VI oocytes (Fig. 8). Microinjection of approximately 50 ng of C11 antibody resulted in substantial CK filament disruption near the site of injection within 2 hr (Fig. 8A), which then spread throughout the entire oocyte by 16–20 hr after injection. Injection of greater amounts (100 ng) of antibody disrupted most CK filaments within 2 hr (not shown). By 18 hr after injection of 50–100 ng of C11 IgG, cytoplasmic CK filaments were nearly completely eliminated (Figs. 8B–8D), with CK filament disruption extending throughout the animal (Fig. 8C), vegetal (Fig. 8D), and perinuclear (not shown) cytoplasm. Disruption of the CK network by the injected antibody was characterized by the loss of CK filaments and the appearance of numerous small CK aggregates within the cytoplasm (Figs. 8C and 8D). Cytoplasmic CK filaments remained disrupted for at least 36 hr (the longest period examined).

Although the cytoplasmic CK filaments were nearly completely eliminated, microinjection of even the highest concentration of C11 antibody (approx. 100 ng of IgG per oocyte) did not completely disrupt the cortical network of CK filaments, even when the postinjection incubation was extended for as long as 36 hr. Cross-sections revealed some CK filaments remaining in both the animal (Fig. 8C) and vegetal (Fig. 8D) cortices of injected oocytes, although the cortical CK network appeared distorted relative to control oocytes. Distorted networks of CK filaments could often be found in grazing optical sections of the lateral and vegetal cortices of oocytes injected with C11 antibodies. The microinjected C11 antibody bound to these distorted cortical CK filaments was readily apparent in fixed oocytes stained with fluorescent anti-mouse IgG (Fig. 8E), indicating that the lack of complete disruption of the cortical CK network did not result from inaccessibility of the cortical CK network.

Normal appearing cytoplasmic and cortical CK networks were observed at all times in uninjected oocytes and in oocytes injected with comparable volumes (50 nl) of buffer

**FIG. 5.** Polarization of the CK filament network is evident in mid stage IV. (A) A low-magnification view of a mid stage IV (600–650 $\mu$m in diameter) oocyte. Note the difference in thickness of the cortical CK network in the animal and vegetal hemispheres.(B) A composite of five images (each a projection of 5 optical sections) spanning the equatorial region of a mid stage IV (800–850 $\mu$m in diameter) oocyte. Note the pronounced difference in cytoplasmic and cortical cytokeratin organization in the animal (upper) and vegetal (lower) regions. CK organization in the animal cortex and cytoplasm is similar to that of fully grown stage VI oocytes. The CK network of the vegetal cortex remains much thicker than that of fully grown stage VI oocytes (compare to Fig. 1). (C) A grazing view (projection of 6 optical sections) of the animal cortex of a mid stage IV (600–650 $\mu$m) oocyte. The organization of CK filaments is similar to that of a fully grown stage VI oocytes. (D) A grazing view (projection of 13 optical sections) of the vegetal cortex of a mid stage IV (600–650 $\mu$m) oocyte. The cortical CK network is much thicker than that observed in fully grown stage VI oocytes. Scale bar is 100 $\mu$m in A and 25 $\mu$m in B and C.
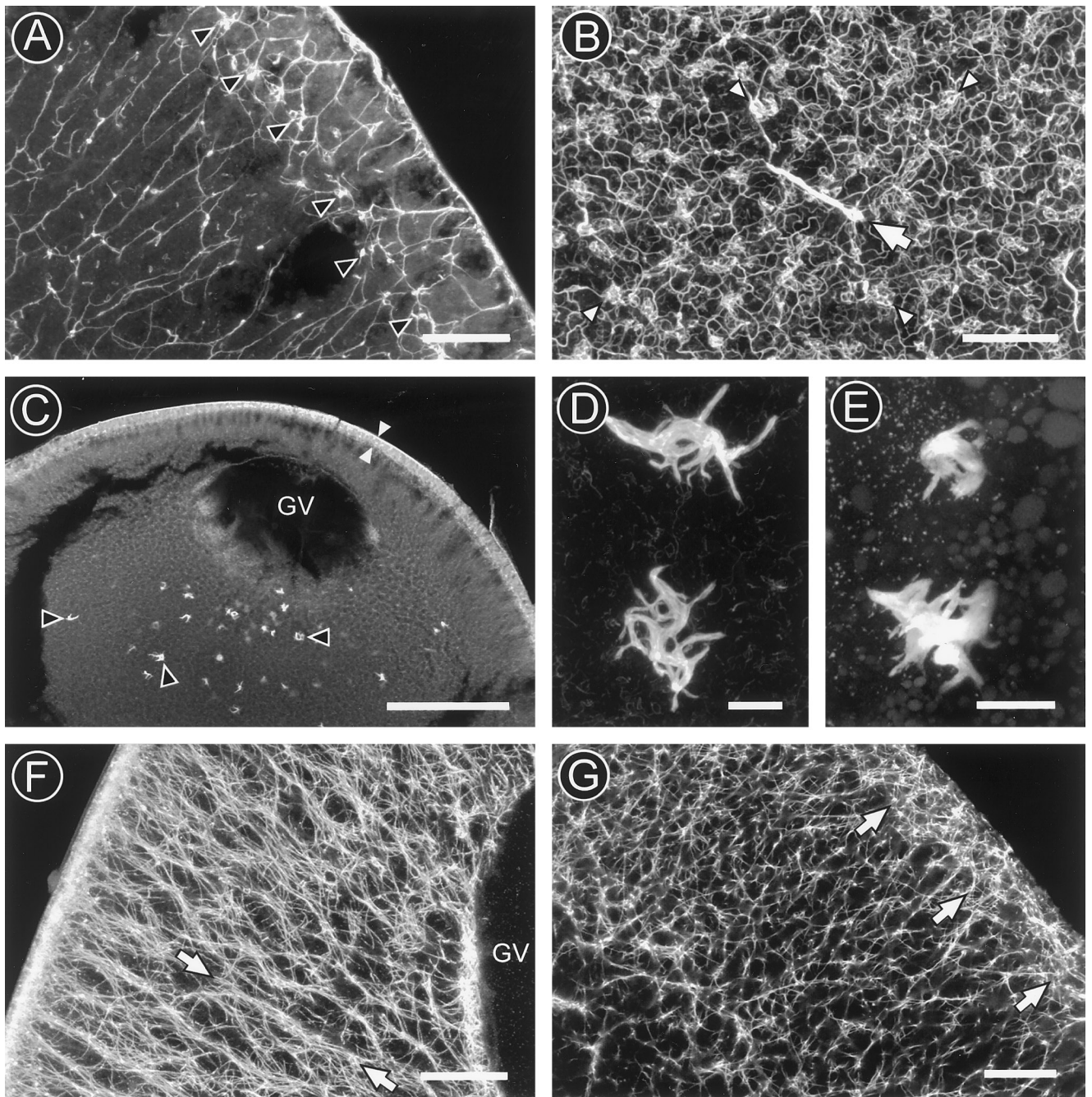
**FIG. 6.** Cytochalasin B disrupts CK filament and MT organization in stage VI *Xenopus* oocytes. (A) Stretching of the cortical CK network into the subcortical cytoplasm (arrowheads) is apparent in the animal hemisphere of an oocyte treated with 20 μg/ml CB for 20 hr (a projection of 5 optical sections). Arrowheads denote the inner margin of the stretched CK network and also point out aggregates of tangled CK filaments. (B) A projection of 13 optical sections of the animal cortex and subcortical cytoplasm of a CB-treated oocyte (20 hr in 20 μg/ml) reveals a large fibrous aggregate (large arrow) and numerous smaller aggregates of tangled CK filaments (small arrowheads). (C) Numerous brightly stained CK aggregates (black arrowheads) are apparent below the GV of this CB-treated oocyte (20 μg/ml CB for 20 hr) stained with C11 antibodies. Note the thickened cortical CK filament network in the animal hemisphere (white arrowheads; compare to Fig.1E). (D) A view of two fibrous CK aggregates in a CB-treated oocyte (20 μg/ml for 41 hr) viewed at higher magnification (a projection of 38 optical sections collected at 1-μm intervals). (E) Similar aggregates in a CB-treated oocytes (20 μg/ml for 20 hr) stained with fluorescein-conjugated phalloidin (a projection of 23 optical sections at 1.5-μm intervals). (F and G) Cross-sectional views of untreated (F) and CB-treated (G) oocytes (20 μg/ml for 40 hr) stained with 6-11B-1 (anti-acetylated α-TB). Arrows in (F) denote radially oriented MT bundles in untreated oocytes. Note the loss of radially oriented MT bundles (arrows in F) and the appearance of a broad cortical region containing disordered MTs (arrows in G) in the CB-treated oocytes. Scale bars are 25 μm in A and B and E and G, 250 μm in C, and 10 μm in F.
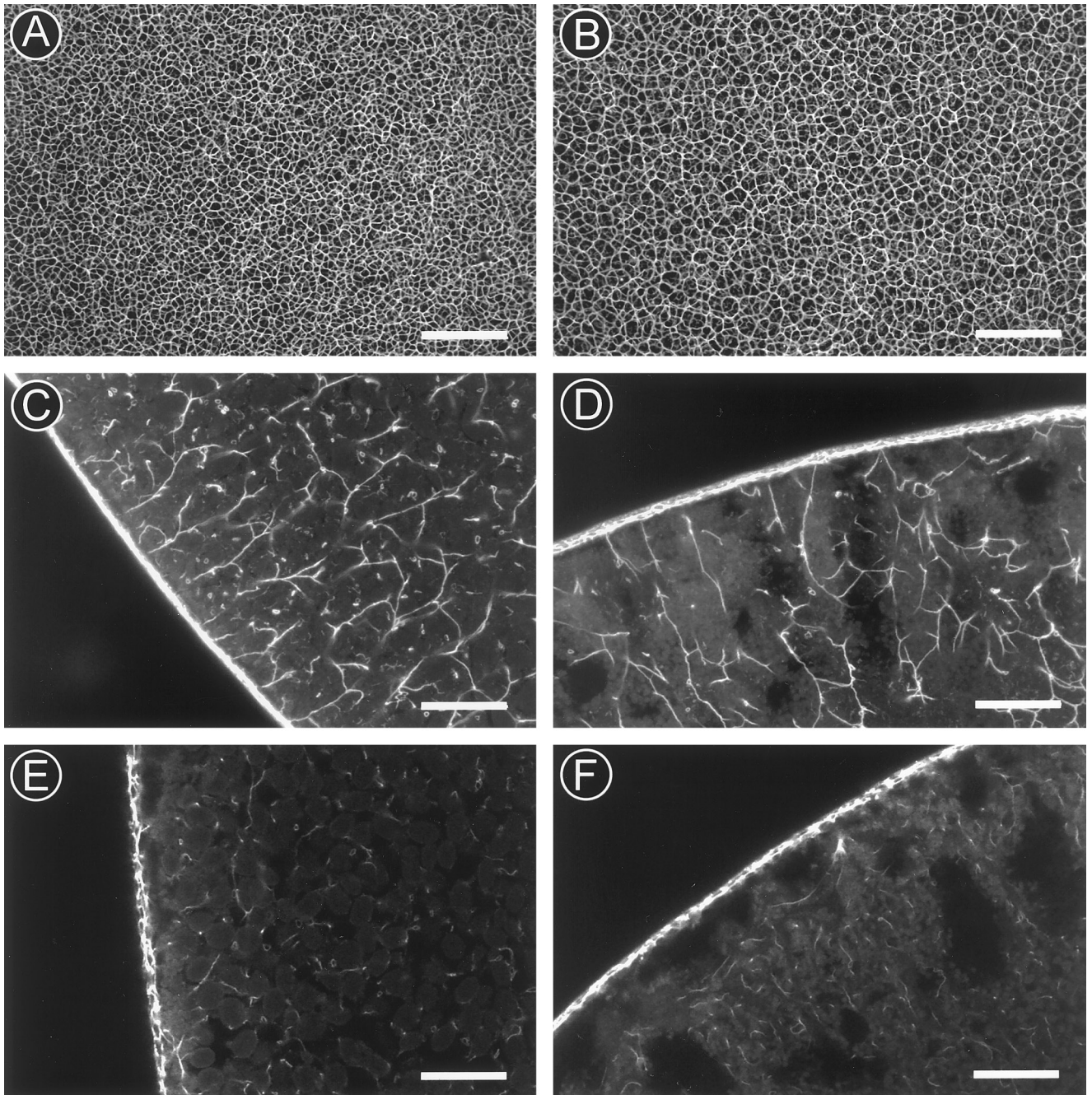
**FIG. 7.** Nocodazole disrupts the A–V polarization of the cortical cytokeratin filament network. (A and B) Grazing views (projections of two and three optical sections, respectively) of the vegetal (A) and animal (B) cortices of oocytes treated for 48 hr with 20 μg/ml NOC, stained with C11 antibodies. Note the fineness of the CK meshwork in the vegetal cortex of NOC-treated cells, relative to the coarser meshwork found in untreated oocytes (compare with Fig. 1A). (C and D) Cross-sectional views (projections of five optical sections) of the vegetal (C) and animal (D) hemispheres of oocytes treated with 20 μg/ml NOC for 48 hr and stained with C11 antibodies. Note the nearly equal thickness of the CK network in the vegetal and animal cortices. (E and F) Cross-sectional views (single optical sections) of the vegetal (E) and animal (F) hemispheres of oocytes treated with a combination of 5 μg/ml NOC and 5 μg/ml CB for 12 hr. Inclusion of NOC inhibits the broadening or stretching of the cortical CK network seen in oocytes treated with CB alone (compare to Figs. 5C and 5D). All scale bars are 25 μm.
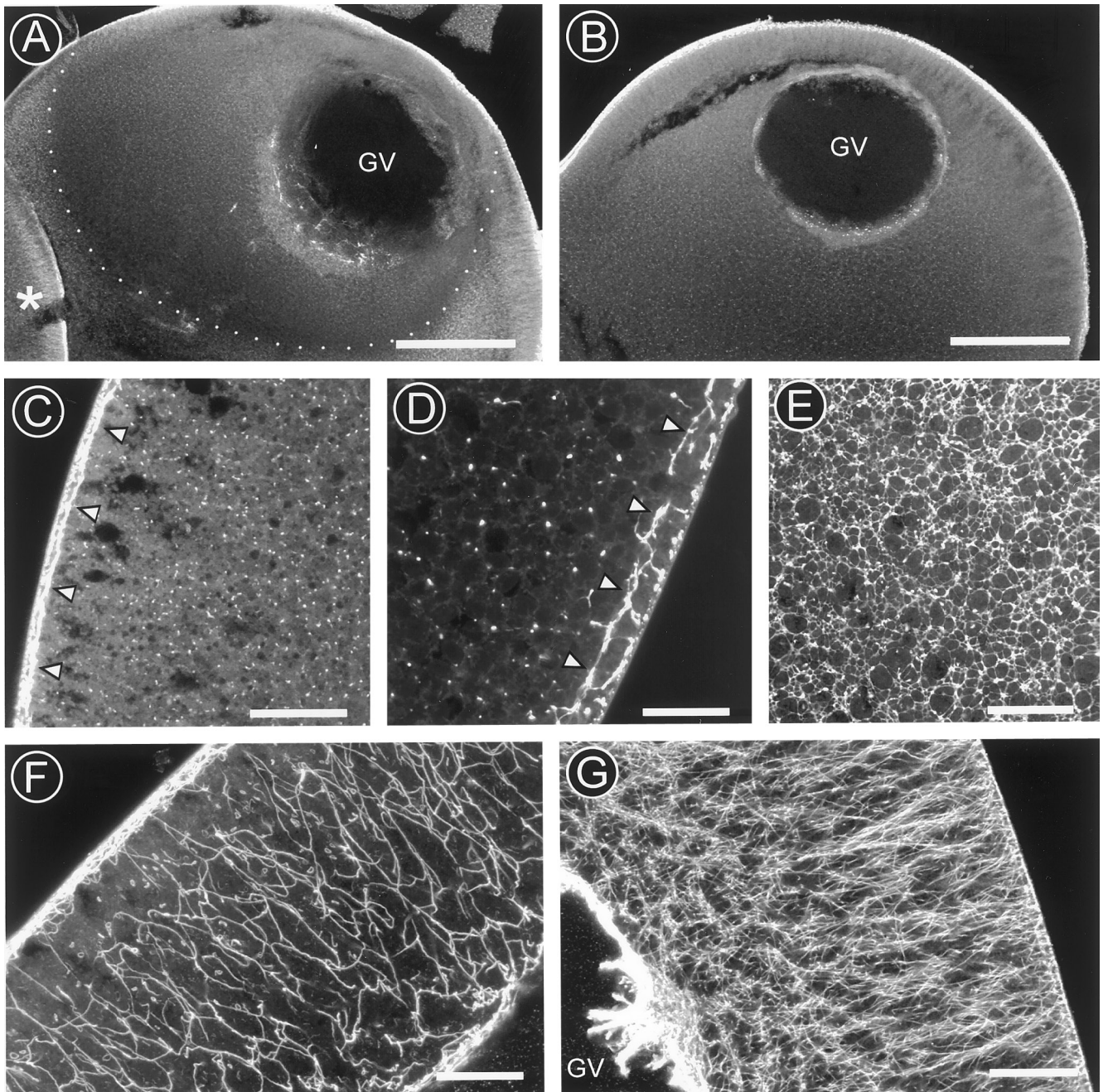
**FIG. 8.** Microinjection of anti-cytokeratin antibodies disrupts cytoplasmic cytokeratin filaments in stage VI *Xenopus.* (A) Low-magnification view (a projection of 5 optical sections at 10-$\mu$m intervals) of an oocyte fixed 2 hr after injection of 50 ng of C11 anti-CK IgG, stained with C11 antibodies. Note the zone of CK filament disruption (dotted outline). Few CK filaments were observed within this zone, while CK filament organization in the surrounding cytoplasm appeared normal. (B) Low-magnification view (a projection of 4 optical sections at 10-mm intervals) of an oocyte fixed 18 hr after injection of 100 ng of C11 IgG, stained with C11 antibodies. Cytoplasmic CK filaments were eliminated nearly completely. (C and D) High-magnification views (C is a single optical section, D is a projection of 5 optical sections; note the difference in scale) of animal (C) and vegetal (D) regions fixed 18 hr after injection of 100 ng of C11 IgG, stained with C11 antibodies. Note the numerous small CK aggregates and remnants of the cortical CK network (denoted by arrowheads in C and D). (E) A view of the vegetal cortex (a projection of 10 optical sections collected at 1-mm intervals) of an oocyte injected with 100 ng of C11 IgG and stained with Texas red-conjugated anti-mouse IgG. Injected antibody is bound to individual CK filaments in the severely distorted cortical CK network. (F) Cortical and cytoplasmic CK filaments were not affected by injection of 50 nl of K glutamate injection buffer (a projections of 10 optical sections). (G) MT organization (stained with anti-$\alpha$-TB) appears normal 24 hr after injection of 100 ng of C11 IgG. Note the characteristic radial bundles of MTs in the animal hemisphere. Scale bars are 250 $\mu$m in A and B, 50 $\mu$m in C, and 25 $\mu$m in D–G.

alone (Fig. 8F) or comparable amounts of anti-tau (500 ng of ascites protein containing approximately 100 ng of IgG) (not shown). Injection of C11 antibodies or injection buffer alone had no effect on progesterone-induced maturation of stage VI oocytes (not shown).

Disruption of the CK networks of stage VI oocytes had no apparent effects on other aspects of cytoplasmic organization, including the distribution of pigment (not shown) and yolk or the position of the GV (compare Figs. 8A and 8B with Fig. 1E). The number and distribution of MTs (both total MTs and those containing acetylated $\alpha$-TB) also appeared unaffected by injection of C11 antibodies for up to 36 hr after injection (compare Fig. 8G with Fig. 6F), despite the substantial disruption of cytoplasmic and cortical CK filaments observed in C11-injected oocytes (see above).

## DISCUSSION

Confocal immunofluorescence microscopy with anti-CK antibodies revealed a continuous network of CK filaments extending throughout the cortex of stage VI *Xenopus* oocytes, including both the vegetal and animal cortices. The anastomosing networks of CK filaments in the vegetal cortex seen in confocal images were similar to those previously observed in whole-mounted oocytes (Klymkowsky *et al.,* 1987) and isolated cortices (Elinson *et al.,* 1993) examined by conventional immunofluorescence microscopy. However, the extensive CK filament network of the animal cortex (apparent in more than 95% of the oocytes examined by confocal microscopy) was not consistently observed or readily apparent in previous studies examining sectioned or whole-mounted oocytes (Franz *et al.,* 1983; Godsave *et al.,* 1984; Klymkowsky *et al.,* 1987; Torpey *et al.,* 1992; Ryabova *et al.,* 1993). Although Elinson *et al.* (1993) observed a network of CK filaments in isolated animal cortices from stage VI oocytes, the distinctive animal–vegetal polarity of the cortical CK network was not apparent in these cortical preparations. A–V polarity was strikingly evident in both the thickness (animal > vegetal) and complexity (animal > vegetal) of the cortical CK filament network apparent in confocal images, providing additional evidence for the structural and functional polarization of the cortical cytoskeleton of stage VI *Xenopus* oocytes (Klymkowsky *et al.,* 1987; Gard, 1993a, 1994; reviewed in Gard, 1995).

The role of the polarized network of CK filaments observed in the cytoplasm and cortex of *Xenopus* oocytes during oogenesis and formation of the A–V axis has been a topic of considerable speculation. The extensive network of CK filaments in the oocyte cortex may contribute to the structural elasticity and integrity of the oocyte cortex. However, the number of radially oriented cytoplasmic CK filaments observed to link the GV to the cortex (estimated to be 9000–15,000 per oocyte) is vastly exceeded by the number of cytoplasmic microtubules (estimated to be 500,000–800,000 per oocyte) (Gard, 1991). Moreover, in contrast to the dramatic effects of disrupting F-actin or MTs on the cytoplasmic organization of stage VI oocytes (Roeder

and Gard, 1994; Gard, 1991, 1993a), disruption of cytoplasmic CK filaments by microinjected anti-CK antibodies had no apparent effect on GV position, or the distribution of yolk or pigment, or the organization of other cytoskeletal systems. It thus appears unlikely that cytoplasmic CK filaments play a major role in maintaining the overall cytoplasmic organization of stage VI *Xenopus* oocytes.

The A–V asymmetry of the cortical CK network (Klymkowsky *et al.,* 1987), combined with the isolation of specific maternal mRNAs from detergent-insoluble CK-rich cytoskeletal fractions (Pondel and King, 1988; Forristall *et al.,* 1995) and isolated cortices (Elinson *et al.,* 1993), has led to proposals that CK filaments in the vegetal cortex play a role in the anchoring of developmentally important maternal mRNAs (Forristall *et al.,* 1995; however, see Klymkowsky and Maynell, 1989; Klymkowsky *et al.,* 1991). Although the precise role of CK filaments in RNA localization and anchoring remains uncertain, the timing of RNA localization relative to assembly and polarization of the CK filament network places some constraints on the potential role of CK filaments in RNA localization (see below).

Figures 9A and 9B outline the organization of CK filaments during key stages of assembly and the polarization of the CK filament network in *Xenopus* oocytes, summarizing results from previously published reports (Franz *et al.,* 1983; Godsave *et al.,* 1984; Klymkowsky *et al.,* 1987; Torpey *et al.,* 1992a; Elinson *et al.,* 1993; Ryabova *et al.,* 1993) and information revealed by confocal immunofluorescence microscopy (this report). CK filaments were not detectable in oocytes during the earliest stages of oogenesis, from mitotic oogonia through early stage I. Assembly of extensive perinuclear, cortical, and cytoplasmic networks of CK filaments was not observed until mid–late stage I (Godsave *et al.,* 1984; this report). This contrasts with the distribution of the two other major cytoskeletal systems, composed of F-actin and MTs, which are both present from the earliest stages of oogenesis (Gard *et al.,* 1995a; Gard, 1991; Roeder and Gard, 1994). Thus, the CK filament network is actually the last of the three major cytoskeletal networks (F-actin, MTs, and CK filaments) to be established in *Xenopus* oocytes.

A complex network of CK filaments was observed to surround and penetrate the mitochondrial mass of stage I oocytes, from their earliest stages of aggregation (Godsave *et al.,* 1984; this report). In this respect, the distribution of CK filaments is similar to that of F-actin cables and MTs, both of which are present in large numbers in the mitochondrial mass of stage I *Xenopus* oocytes (Gard, 1991; Gard *et al.,* 1995a; Roeder and Gard, 1994). However, no evidence of regional specialization of the CK filament network (this report), F-actin distribution (Roeder and Gard, 1994), or MT distribution (Gard, 1991; Gard *et al.,* 1995a) that might structurally correspond to the RNA transport organizer described by Kloc and Etkin (1995) was apparent within the mitochondrial mass.

Aside from the concentration of CK filaments surrounding and within the mitochondrial mass during stage I–II, there was no evidence of asymmetry in the distribution
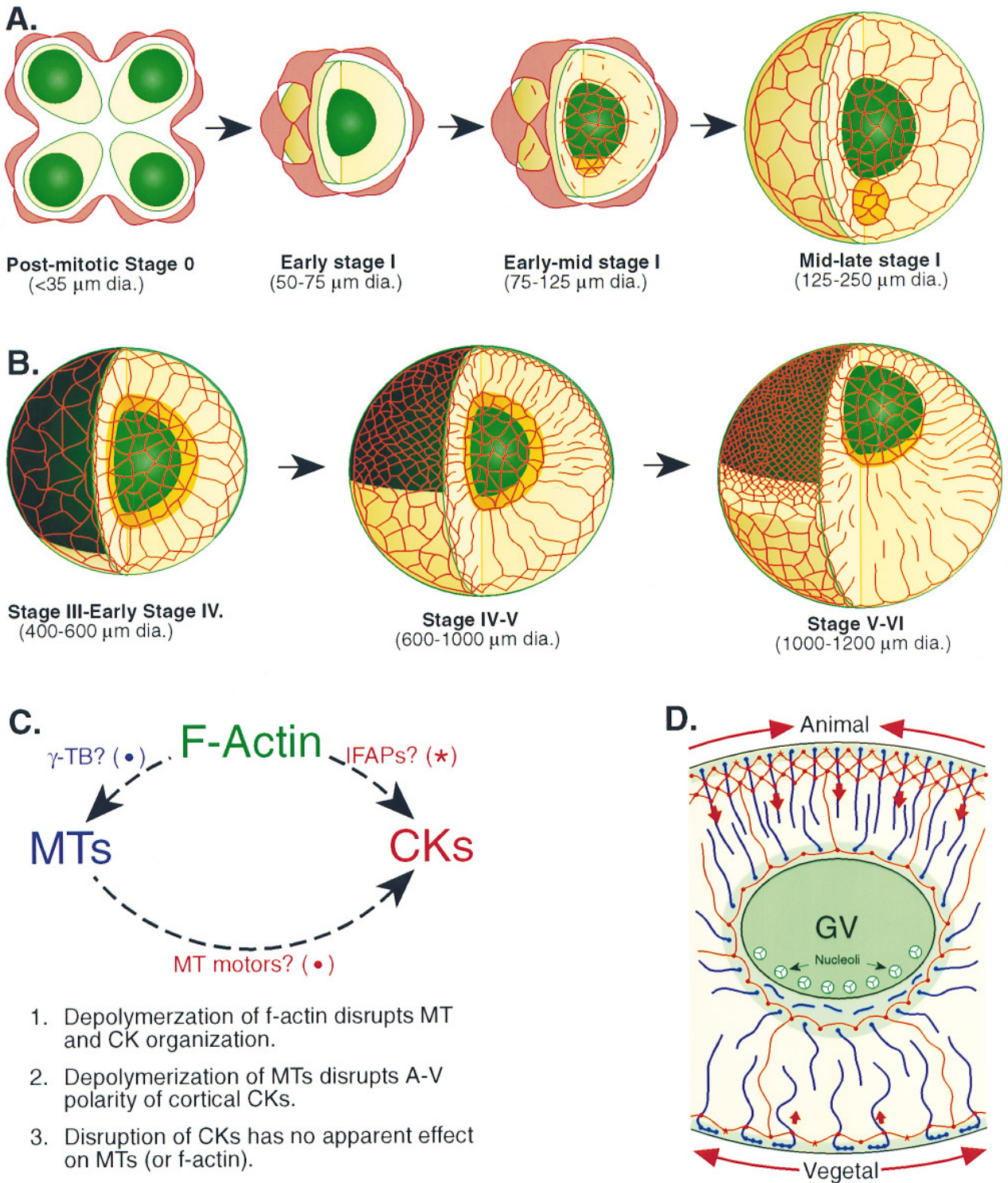
**FIG. 9.** A summary of cytokeratin filament and cytoskeletal organization and polarization during oogenesis in *Xenopus laevis*. (A) During stage 0 and early stage I, oocytes lack CK filaments, which are found in the surrounding follicle cells. By early–mid stage I, CK filaments form a network surrounding the GV, surround and penetrate the mitochondrial mass, and begin to extend into the cytoplasm. By mid–late-stage I, an extensive network of cytoplasmic CK filaments links the perinuclear network to the mitochondrial mass and cortex. (B) CK filaments are symmetrically distributed during early stage IV. Polarization of the cortical and cytoplasmic CK filament networks is apparent during mid stage IV–stage V, as first the animal (during mid stage IV) and then the vegetal (during stage V) CK filament networks adopt the organization characteristic of stage VI. Summarized from Franz *et al.* (1983); Godsave *et al.* (1984), Klymkowsky *et al.* (1987);

of CK filaments (including the perinuclear network and the cytoplasmic and cortical CK filaments) during the early stages of oogenesis (stages I–early stage IV). Polarization of the CK filament network was not apparent until mid stage IV, well after the A–V axis became evident by the unequal distribution of pigment. Previous reports have indicated that maternal RNAs (both mRNAs and noncoding transcripts) are localized to the presumptive vegetal cortex during stages II–early IV of oogenesis (Yisraeli *et al.,* 1990; Forristall *et al.,* 1995; Kloc and Etkin, 1995), indicating that A–V polarization of the CK network occurs subsequent to the period in which maternal RNAs are being transported and localized to the oocyte cortex. It is unlikely, then, that asymmetry of the CK filament network contributes to the targeting of maternal transcripts to the vegetal cortex. However, CK filaments may play a role in the localization of maternal mRNAs to the cortex during stages II–IV of oogenesis, and subsequent polarization of the cortical CK network could affect the final distribution of maternal mRNAs or other components in the cortex (see below).

Although MTs, F-actin, and CK filaments each have a characteristic spatial and temporal organization during oogenesis, there is considerable overlap in their spatial distribution within the cytoplasm of stage VI *Xenopus* oocytes. Together with preliminary studies of the effects of cytoskeletal inhibitors on stage VI oocytes (Roeder and Gard, 1994; Cha and Gard, unpublished observations; Gard *et al.,* 1995b; Klymkowsky, 1995), these have led to speculation that the three cytoskeletal networks might interact structurally (Klymkowsky, 1995; Gard, 1995). The data presented in this report strengthen this conclusion and further suggest that the organization and A–V polarization of the oocyte cytoskeleton is dependent upon a hierarchy of interactions among F-actin, MTs, and CK filaments.

First, a subset CK filaments appears to be released from the cortex and pulled into the subcortical cytoplasm of CB-treated stage VI oocytes. Although release of cortical CK filaments in CB-treated oocytes was not complete, previous studies indicated that disruption of the cortical actin cytoskeleton by CB was also incomplete, even after prolonged treatment (Roeder and Gard, 1994). Thus, it remains possible that linkage of the CK filament network to the cortex is entirely dependent upon cortical actin. Alternatively, a subset of CK filaments may be anchored in the cortex through actin-independent linkages.

Numerous aggregates of CK-containing filaments were also apparent in the cytoplasm of CB-treated oocytes, suggesting that F-actin plays a role in the organization of cytoplasmic and cortical CK filaments, as well. These aggregates of CK filaments are reminiscent of vimentin filament aggregates observed in cultured cells treated with MT inhibitors (reviewed in Klymkowsky *et al.,* 1989). However, unlike vimentin, aggregation of CK filaments has not been previously observed in epithelial cells treated with either MT or actin inhibitors, suggesting that the mechanisms responsible for maintaining CK filament organization in oocytes and epithelial cells are distinct. The similarities in morphology and distribution of cytoplasmic aggregates in CB-treated oocytes stained with anti-CK antibodies or fluorescein phalloidin suggest that CK filaments and residual F-actin coaggregate, providing additional evidence for an intimate association between the actin and CK filament systems.

Treatment with CB also disrupted MT organization in stage VI *Xenopus* oocytes (Roeder and Gard, 1994, Cha and Gard, unpublished observations, Gard *et al.,* 1995c; this report), indicating that MT organization is dependent upon F-actin. The broadening of the cortical MT array and the loss of radial MT organization seen in CB-treated oocytes are consistent with a model in which F-actin-dependent linkages to the oocyte cortex play a major role in maintaining MT organization and polarity. Interestingly, $\gamma$-tubulin, a centrosomal protein localized to the cortex of stage VI *Xenopus* oocytes, is also released from the cortex in CB-treated oocytes (Gard, 1994; Gard and Becker, unpublished observations), suggesting that $\gamma$-TB might link the MT cytoskeleton to F-actin in the oocyte cortex. Alternatively, MTs and F-actin may be linked through complexes of cytoplasmic dyneins and dynactin, which have been proposed to link MTs of spindle asters to cortical actin in a number of cell types (Clark and Meyer, 1994; Muhua *et al.,* 1994; Schroer, 1994; Waterman-Storer *et al.* 1995). Together with reports that F-actin is required for the anchoring of maternal RNAs (Yisraeli *et al.,* 1990; Kloc and Etkin, 1995), these results indicate that actin microfilaments play a critical role in the organization of the cortex of *Xenopus* oocytes. However, they also suggest that caution must be used in interpreting the effects of CB on the localization of developmentally important mRNAs, since CB affects the organization of all elements of the oocyte cytoskeleton.

Treatment with microtubule inhibitors such as nocodazole, colcemid, and vinblastine also had a dramatic effect on CK filament organization in stage VI *Xenopus* oocytes,

Torpey *et al.* (1992), Ryabova *et al.* (1993), and this report. (C) Organization and polarization of the CK filament cytoskeleton in stage VI *Xenopus* oocytes are dependent upon both F-actin and MTs: (1) CK filament organization is dependent upon cortical and cytoplasmic F-actin; (2) MT organization is dependent upon F-actin; (3) polarization of the cortical cytokeratin network is dependent upon MTs; but (4) neither MT nor actin organization is dependent upon cytoplasmic cytokeratin filaments. (D) A model for the organization of the cytoskeleton of stage VI *Xenopus* oocytes. MTs (blue lines) are anchored to cortical and perinuclear actin (green) via the centrosomal protein $\gamma$-TB (blue dots). Cytokeratin filaments (red lines) are anchored to F-actin in the cortical and perinuclear cytoplasm by an unidentified protein complex (red *). Cytokeratins are also linked to MTs, possibly by a MT-dependent motor protein. Cytoplasmic actin cables have been omitted for clarity. In this model, the A–V polarity of the MT cytoskeleton is specified by the asymmetric distribution of the centrosomal protein $\gamma$-TB in the oocyte cortex, and the A–V polarity of the cortical cytokeratin network is dependent upon the asymmetric organization of MTs in the animal and vegetal hemispheres (see text).

nearly eliminating the characteristic A–V asymmetry of the cortical CK filament network. Polarity of the cortical CK network thus appears to be highly dependent upon intact microtubules. Moreover, combined treatment with NOC and CB inhibited the inward stretching of cortical CK filaments induced by CB alone, suggesting that MTs generate an inward tension on the cortical CK filament network.

Despite the dependence of CK filament organization on both F-actin and MTs, nearly complete elimination of the cytoplasmic network of CK filaments and substantial distortion of the cortical CK network of stage VI oocytes by microinjected antibodies had no apparent effect on the organization of oocyte MTs. Disruption of the CK filament network also had no apparent effect on cytoplasmic organization, including the position of the GV and the distribution of yolk and pigment. In combination with the observed dependence of MT organization and GV position on F-actin (Roeder and Gard, 1994; Gard *et al.,* 1995c; Cha and Gard, unpublished observations; this report), these results suggest that the organization of F-actin is also largely independent of the CK cytoskeleton.

The nature of the linkage between CK filaments and the MT and actin cytoskeletons of *Xenopus* oocytes remains to be identified. Studies of IF–MT interactions in cultured cells and *in vitro* have suggested that MT-associated proteins (MAPs) or members of the kinesin family of MT-dependent motors might link IFs to MTs (Flynn and Purich, 1987; Hermann *et al.,* 1985, Leterrier *et al.,* 1982; Gyoeva and Gelfand, 1991). Recently, members of a family of related intermediate filament-associated proteins (IFAPs), which includes plectin, desmoplakin, and bullous pemphigoid antigen (BPAG), have been proposed as linkers between intermediate filaments and both the actin and MT cytoskeletons in mammalian cells (Green *et al.,* 1992; Siefert *et al.,* 1992; Wiche *et al.,* 1993; Foisner *et al.,* 1995; Yang *et al.,* 1996). All of these proteins (MAPs, MT motors, and IFAPs) are potential mediators of the proposed interactions between CK filaments and the MT and actin cytoskeletons in *Xenopus* oocytes.

From these observations, we conclude that the establishment and maintenance of the polarized oocyte cytoskeleton are dependent upon a hierarchy of interactions among F-actin, MTs, and CKs, which are summarized in Fig. 9C: (1) MT and CK filament organization is dependent upon F-actin; (2) A–V polarization of the cortical CK network is dependent upon MTs; and (3) MT and F-actin organization is largely independent of CK filaments. A model summarizing the interactions among CK filaments, MTs, and F-actin in stage VI oocytes is shown in Fig. 9D. In this model, inward tension generated by the numerous radially oriented MTs of the animal hemisphere pull the cortical CK filaments (which are anchored to cortical F-actin) inward, forming the three-dimensional network characteristic of the animal cortex. A–V differences in MT number and organization also cause the cortical CK filaments to ''bunch up'' in the animal cortex and laterally stretch the CK network of the vegetal cortex toward more animal regions of the cortex to form the more open CK filament meshwork characteris-

tic of the vegetal cortex. In this model, the A–V polarity of the cortical CK network results directly from A–V asymmetry in the organization of cytoplasmic MTs (Gard, 1991; Gard *et al.,* 1995c). This model could also provide a cytoskeletal basis for the lateral spread of localized components in the vegetal cortex during the later stages of oogenesis, including maternal mRNAs that play important roles in later embryonic development (Kloc and Etkin, 1995).

## ACKNOWLEDGMENTS

## REFERENCES

Al-Mukhtar, K. A. K., and Webb, A. (1971). An ultrastructural study of primordial germ cells, oogonia, and early oocytes in *Xenopus laevis. J. Embryol. Exp. Morphol.* **26,** 195–217.

Bartek, J., Vojtesek, B., Staskova, Z., Bartkova, J., Kerekes, Z., Rejthar, A., and Kovarik, J. (1991). A series of 14 new monoclonal antibodies to keratins: Characterization and value in diagnostic histopathology. *J. Pathol.* **164,** 215–224.

Clark, S. W., and Meyer, D. I. (1994). ACT3: A putative centractin homologue in *S. cerevisiae* is required for proper orientation of the mitotic spindle. *J. Cell Biol.* **127,** 129–138.

Coggins, L. W. (1973). An ultrastructural and autoradiographic study of early oogenesis in the toad: *Xenopus laevis. J. Cell Sci.* **12,** 71–93.

Coleman, A., Morser, J., Lane, C., Besley, J., Wylie, C., and Valle, G. (1981). Fate of secretory proteins trapped in oocytes of *Xenopus laevis* by disruption of the cytoskeleton or by imbalanced subunit synthesis. *J. Cell Biol.* **91,** 770–778.

Dumont, J. (1972). Oogenesis in *Xenopus laevis* (Daudin). I. Stages of oocyte development in laboratory maintained animals. *J. Morphol.* **136,** 153–180.

Elinson, R. P., King. M. L., and Forristall, C. (1993). Isolated vegetal cortex from *Xenopus* oocytes selectively retains localized mRNAs. *Dev. Biol.* **160,** 554–562.

Foisner, R., Bohn, W., Mannweiler, K., and Wiche, G. (1995). Distribution and ultrastructure of plectin arrays in subclones of rat glioma $C_6$ cells differing in intermediate filament protein (vimentin) expression. *J. Struct. Biol.* **115,** 304–317.

Flynn, G., and Purich, D. (1987). GTP regeneration influences interactions of microtubules, neurofilaments, and microtubule-associated proteins *in vitro. J. Biol. Chem.* **262,** 15443–15447.

Forristall, C., Pondel, M., Chen, L., and King, M. L. (1995). Patterns of localization and cytoskeletal association of two vegetally-localized RNAs Vg1 and Xcat2. *Development* **121,** 201–208.

Franke, W. W., Rathke, P. C., Seib, E., Trendelenberg, M. F., Osborn, M., and Weber, K. (1976). Distribution and mode of arrangement of microfilamentous structures and actin in the cortex of amphibian oocytes. *Cytobiologie* **14,** 111–130.

Franz, J. K., Gall, L., Williams, M. A., Picheral, B., and Franke, W. W. (1983). Intermediate-sized filaments in a germ cell: Expression of cytokeratins in oocytes and eggs of the frog *Xenopus. Proc. Natl. Acad. Sci. USA* **80,** 6254–6258.

Franz, J. K., and Franke, W. W. (1986). Cloning of a cDNA and amino acid sequence of a cytokeratin expressed in oocytes of *Xenopus laevis. Proc. Natl. Acad. Sci. USA* **83,** 6475–6479.

Gard, D. L. (1991). Organization, nucleation, and acetylation of microtubules in *Xenopus laevis* oocytes: A study by confocal immunofluorescence microscopy. *Dev. Biol.* **143,** 346–362.

Gard, D. L. (1993a). Ectopic spindle assembly during maturation of *Xenopus* oocytes: Evidence for functional polarization of the oocyte cortex. *Dev. Biol.* **159,** 298–310.

Gard, D. L. (1993b). Confocal immunofluorescence microscopy of microtubules in amphibian oocytes and eggs. *Methods Cell Biol.* **38,** 241–264.

Gard, D. L. (1994). γ-Tubulin is asymmetrically distributed in the cortex of *Xenopus* oocytes. *Dev. Biol.* **161,** 131–140.

Gard, D. L. (1995). Axis formation during amphibian oogenesis: Reevaluating the role of the cytoskeleton. *Curr. Topics Dev. Biol.* **30,** 215–252.

Gard, D. L., Affleck, D., and Error, B. M. (1995a). Microtubule organization, acetylation, and nucleation in *Xenopus laevis* oocytes. II. A developmental transition in microtubule organization during early diplotene. *Dev. Biol.* **168,** 189–201.

Gard, D. L., Cha, B. J., and Roeder, A. D. (1995b). F-actin is required for spindle anchoring and rotation in *Xenopus* oocytes: A reexamination of the effects of cytochalasin B on oocyte maturation. *Zygote* **3,** 17–26.

Gard, D. L., Cha, B.-J., and Schroeder, M. M. (1995c). Confocal immunofluorescence microscopy of microtubules, microtubule-associated proteins, and microtubule-organizing centers during amphibian oogenesis and early development. *Curr. Topics Dev. Biol.* **31,** 383–431.

Gard, D. L., and Kirschner, M. (1987). A microtubule-associated protein from *Xenopus* eggs that specifically promotes assembly at the plus-end. *J. Cell Biol.* **105,** 2203–2215.

Gerhart, J. C. (1980). Mechanisms regulating pattern formation in the amphibian egg and early embryo. *In* ''Biological Regulation and Development'' (R. F. Goldberger, Ed.), pp. 133–316. Plenum, New York.

Godsave, S. F., Wylie, C. C., Lane E. B., and Anderton, B. H. (1984). Intermediate filaments in the *Xenopus* oocyte: The appearance and distribution of cytokeratin-containing filaments. *J. Embryol. Exp. Morphol.* **83,** 157–167.

Green, K. J., Virata, M. L., Elgart, G. W., Stanley, J. R., and Parry, D. A. (1992). Comparative structural analysis of desmoplakin, bullous pemphigoid antigen, and plectin: Members of a new gene family involved in the organization of intermediate filaments. *Int. J. Biol. Macromol.* **14,** 145–153.

Goldman, R. D., and Steinert, P. M. (Eds.) (1990) ''Cellular and Molecular Biology of Intermediate Filaments.'' Plenum, New York.

Gyoeva, F. K., and Gelfand, V. I. (1991). Coalignment of vimentin intermediate filaments and microtubules depends upon kinesin. *Nature* **353,** 445–448.

Herman, R., Shelanski, M., and Liem, R. (1985). Microtubule-associated proteins bind specifically to the 70 kDa neurofilament protein. *J. Biol. Chem.* **260,** 12160–12166.

Huchon, D. Jessus, C. Thibier, C., and Ozon, R. (1988). Presence of microtubules in isolated cortices of prophase I and metaphase II oocytes in *Xenopus laevis. Cell Tissue Res.* **154,** 415–420.

Kloc, M., and Etkin, L. D. (1995). Two distinct pathways for the localization of RNAs at the vegetal cortex in *Xenopus* oocytes. *Development* **121,** 287–297.

Klymkowsky, M. W. (1995). Intermediate filament organization, reorganization, and function in the clawed frog *Xenopus. Curr. Topics Dev. Biol.* **31,** 455–486.

Klymkowsky, M. W., Bachant, J. B., and Domingo, A. (1989). *Cell Motil. Cytoskeleton* **14,** 309–331.

Klymkowsky, M. W., and Maynell, L. A. (1989). MPF-induced breakdown of cytokeratin filament organization in maturing *Xenopus* oocytes depends on the translation of maternal mRNAs. *Dev. Biol.* **134,** 479–485.

Klymkowsky, M. W., Maynell, L. A., and Nislow, C. (1991). Cytokeratin phosphorylation, cytokeratin filament severing, and the solubilization of the maternal mRNA Vg1. *J. Cell Biol.* **114,** 787–797.

Klymkowsky, M. W., Maynell, L. A., and Polson, A. G. (1987). Polar asymmetry in the organization of the cortical cytokeratin system of *Xenopus laevis* oocytes and embryos. *Development* **100,** 543–557.

Klymkowsky, M. W., Miller, R. H., and Lane, E. B. (1983). Morphology, behavior, and interactions of cultured epithelial cells after the antibody-induced disruption of keratin filament organization. *J. Cell Biol.* **96,** 494–509.

Klymkowsky, M. W., Shook, D. R., and Maynell, L. A. (1992). Evidence that the deep cytokeratin filament systems of the *Xenopus* embryo act to ensure normal gastrulation. *Proc. Natl. Acad. Sci. USA* **89,** 8736–8740.

Leterrier, J.-F., Liem, R., and Shelanski, M. (1982). Interactions between neurofilaments and microtubule-associated proteins: A possible mechanism for intra-organellar bridging. *J. Cell Biol.* **95,** 982–986.

Muhua, L., Karpova, T. S., and Cooper, J. A. (1994). A yeast actin-related protein homologous to that in vertebrate dynactin complex is important for spindle orientation and nuclear migration. *Cell* **78,** 669–679.

Palecek, J. Habrova, V., Nedvidek, J., and Romanovsky, A. (1985). Dynamics of tubulin structures in *Xenopus laevis* oogenesis. *J. Embryol. Exp. Morphol.* **87,** 75–86.

Piperno, G., LeDizet, M., and Chang, X.-J. (1987). Microtubules containing acetylated α-tubulin in mammalian cells in culture. *J. Cell Biol.* **104,** 289–302.

Pondel, M., and King, M. L. (1988). Localized maternal mRNA related to transforming growth factor β mRNA is concentrated in a cytokeratin-enriched fraction from *Xenopus* oocytes. *Proc. Natl. Acad. Sci. USA* **85,** 7612–7616.

Reynolds, E. S. (1963). The use of lead citrate at high pH as an electron-opaque stain in electron microscopy. *J. Cell Biol.* **17,** 208–212.

Roeder, A. D., and Gard, D. L. (1994) Confocal microscopy of F-actin distribution in *Xenopus* oocytes. *Zygote* **2,** 111–124.

Ryabova, L. V., Betina, M. I., and Vassetzky, S. G. (1986). Influence of cytochalasin B on oocyte maturation in *Xenopus laevis. Cell Differ.* **19,** 89–96.

Ryabova, L. V., Virtanen, I., Lehtonen, E., Wartiovaara, J., and Vassetzky, S. G. (1993). Morphology of the keratin cytoskeleton of *Xenopus* oocytes as studied using heterologous monoclonal antibodies. *Russ. J. Dev. Biol.* **24,** 364–372.

Schroer, T. A. (1994). New insights into the interaction of cytoplasmic dynein with the actin-related protein, Arp1. *J. Cell Biol.* **127,** 1–4.

Schulze, E., Asai, D. J., Bulinski, J. C., and Kirschner, M. W. (1987). Post-translational modification and microtubule stability. *J. Cell Biol.* **105,** 2167–2177.

Seifert, G. J., Lawson, D., and Wiche, G. (1992). Immunolocalization of the intermediate filament-associated protein plectin at focal contacts and actin stress fibers. *Eur. J. Cell Biol.* **59,** 138–147.

Staskova, Z., Vojtesek, B., Lukas, J., Pavlovska, R., Kamenicka,

T., Kovarik, J., and Bartek, J. (1991). Phylogenetically-conserved epitopes of the keratin 8 polypeptide recognized by a novel set of monoclonal antibodies. *Folia Biol.* **37,** 197–206.

Torpey, N. P., Heasman, J., and Wylie, C. C. (1992a). Distinct distribution of vimentin and cytokeratin in *Xenopus* oocytes and early embryos. *J. Cell Sci.* **101,** 151–160.

Torpey, N., Wylie, C. C., and Heasman, J. (1992b). Function of maternal cytokeratin in *Xenopus* development. *Nature* **357,** 413–415.

Waterman-Storer, C. M., Karki, S., and Holzbaur, E. L. (1995). The p150^Glued component of the dynactin complex binds to both microtubules and the actin-related protein centractin (Arp-1). *Proc. Natl. Acad. Sci. USA* **92,** 1634–1638.

Webster, D. R., and Borisy, G. G. (1989). Microtubules are acetylated in domains that turn over slowly. *J. Cell Sci.* **92,** 57–65.

Wiche, G., Gromov, D., Donovan, A, Castanon, M. J., and Fuchs, E. (1993). Expression of plectin mutant cDNA in cultured cells indicates a role of COOH-terminal domain in intermediate filament association. *J. Cell Biol.* **121,** 607–619.

Wylie, C. C., Brown, D., Godsave, S., Quarmby, J., and Heasman, J. (1985) The cytoskeleton of *Xenopus* oocytes and its role in development. *J. Embryol. Exp. Morphol. (Suppl.)* **89,** 1–15.

Yang, Y., Dowling, J., Yu, Q.-C., Kouklis, P., Cleveland, D., and Fuchs, E. (1996). An essential cytoskeletal linker protein connecting actin microfilaments to intermediate filaments. *Cell* **86,** 655–665.

Yisraeli, J. K., Sokol, S., and Melton, D. A. (1990). A two step model for the localization of maternal mRNA in *Xenopus* oocytes: Involvement of microtubules and microfilaments in translocation and anchoring of Vg1 mRNA. *Development* **18,** 289–298.